A NON-ENZYMATIC CONTINUOUS GLUCOSE MONITORING SYSTEM USING ELECTROCHEMICAL IMPEDANCE SPECTROSCOPY

by

Sean Moore, B.S.

A thesis submitted to the Graduate Council of
Texas State University in partial fulfillment
of the requirements for the degree of
Master of Science
with a Major in Technology Management
December 2016

Committee Members:

In-Hyouk Song, Chair

Byoung Hee You

Namwon Kim

FAIR USE AND AUTHOR'S PERMISSION STATEMENT

Fair Use

Duplication Permission

DEDICATION

For my past, my present, and my future. To my family.

ACKNOWLEDGEMENTS

I would like to thank my advisor, Dr. In-Hyouk Song. The nature of research is one of stress and turmoil, but his devotion to the advancement of my knowledge provided a spark that fueled an unyielding pursuit for answers. It is truly a privilege to work with a mentor of his caliber as an undergraduate student as well as a graduate student. I also would like to thank Dr. Byoung Hee You and Dr. Namwon Kim. Their diverse knowledge of the field, research techniques, and continuous encouragement were invaluable throughout the entire process and I sincerely thank them for not only serving on my committee, but for all of their help over the years.

To my friends in the micro/nano fabrication laboratory the technology staff, and the biology department. Dr. Juan Gomez, Dr. Sooyeon Park, Mr. Devanda Lek, Dr. Hong-Gu Kang, Yogendra, Mr. Shane Arabie, and Dr. Casey Smith: the many late nights spent running experiments, calibrating equipment, discussing results, and accomplishing our own respective goals are priceless to me. Over the years and more than a few beers, you have all have become some of my closest friends whom I will always recall fondly. Semper Fidelis.

Lastly and most importantly, I must thank my dear wife Marissa. Without her love, none of the work I have accomplished as a student would be possible. It will always be her encouragement, love, and devotion that drive me to do better in all aspects of life. No matter where I am, in good times or bad, I can always look to her and find my way. She is truly my stars, and I can never thank her enough.

TABLE OF CONTENTS

Page

LIST OF TABLES

Table **Page**

LIST OF FIGURES

Figure **Page**

ABSTRACT

The following research is a feasibility trial for the development of a continuous glucose monitoring system using electrochemical impedance spectroscopy. Three separate experiments are conducted to determine the effects of electrode surface area on sensing efficacy, the effects of glucose concentration on impedimetric response, and a real time measuring trial of glucose sensing at low, medium, and high concentration levels over a period of fixed frequency and voltage excitation. The resultant data from each of the trials is modeled using electrical equivalent circuits and analyzed via Nyquist and Bode configurations to identify relevant data for each experiment. Results indicate that as electrode surface area increases, the impedimetric response decreases and sensitivity is increased. Deviations throughout the entire glucose range are detected as an inverse of the impedance in the cell due to the inverse relationship of glucose concentration and charge transfer resistance. The continuous monitoring of glucose is demonstrated by a rapid device response over two iterations of glucose concentration in ascending order. As concentration increases, resolution of the impedance signature is reduced suggesting the approach of a saturation set point.

I. INTRODUCTION

The advancement of point-of-care-diagnostics and monitoring is modernizing the health care industry. Accurate, rapid analysis of analytes using simplistic user interfaces enables the patient to discern their own health status eliminating costly laboratory analysis, physician appointments, and excessive wait times [1]. Recent developments in the fields of microfluidics and MEMS fabrication technologies drive rapid advancements in device miniaturization ensuring portability and facile analysis techniques.

A common goal in the microfluidics community is the replacement of conventional macro-scale assays aligning well with the primary intent of standardized point-of-care-diagnostics. In the past decade, microfluidic lab-on-a-chip (LOC) technology has shown considerable promise in the field of biological testing. The precise control and manipulation of microliter quantities of bio-fluids enable the replacement of a variety of macro scale tests for disciplines that require in-situ flow technologies such as point-of-care-diagnostics, biomimetic systems, and in-vitro monitoring. Thus, microfluidic devices are ideal candidates for a seamless integration with biosensing technology.

1.1 Biosensors

At the intersection of biological and engineering sciences lies biosensor research, a promising field that has become crucial to modern life. Defined as any device that incorporates biological, biologically derived, or biomimetic technology with a transducing element, biosensor research cascades into seemingly astronomical variations that meet the requirements of many fields including diagnostics, food safety and processing, environmental monitoring, biomedicine, and drug discovery [2]. Despite their

complexities, biosensing systems are typically composed of three elements: the analyte such as food samples, human samples, environmental samples, or cell cultures; the transducer, a biological mediator; and a digital interpretation method that consisting of a signal amplifier, processor, and display interface. Biosensors are intrinsically designed to be highly selective enabling customization of the device to a unique biological reaction by implementing specific mediators (biological elements) that have a binding affinity with the target molecule [3]. Since Clark and Lyons pioneered the first generation of glucose sensors implementing glucose oxidase enzymes to detect variations in glycemic index in 1962, biodetection and monitoring have become increasingly complex [4]. Biosensors are roughly divided into two categories, labeled and label-free. Labeled detection requires target molecules or cells to be "labeled" or doped with dyes, chemicals, or any other means to highlight them in solution.

While labeled detection methods are known for their accuracy and reliability, they also typically require costly characterization techniques and specific binding events limiting their applications to laboratory environments [5]. Label-free detection methods enable detection of molecules and cells without the necessity of marking them. Label-free biosensors have a variety of detection mechanisms making them ideal candidates for commercialization as they are inexpensive, simple to manufacture, and easily miniaturized for portability [6]. As research continues to progress a multitude of sensing modes are being developed such as optical, mechanical, electrochemical, or a combination of the three [6].

1.2 Types of Biosensors

Optical biosensors implement the changes in refraction index local to the sensing surface induced by the addition of an analyte [7]. The transducer observes and collects any

local changes in refractive index at the surface of the sensor as a result of the chemical bonding between the analyte and bioreceptor. Since the transducer only detects changes in refactive index local to the sensing surface where target molecules are captured by the bioreceptor, optical methods neglect the presences of unbound analyte or foreign molecules suspended in solution. In addition, sensing surfaces are coated with optical thin films that are often easily contaminated by radicals in solution or damaged in use demanding frequent recalibration, maintenance, and replacement thus hindering their use outside of controlled environments.

Based on atomic force microscopy theory, mechanical biosensors can also provide an accurate means of detection. Microcantilever technology is a proven means of assay for a variety of analytes including antigens, proteins, bacteria, pathogens, ions, and DNA [8]. In mechanical biosensors, molecules that can selectively immobilize a target are suspended in solution and used to coat one side of a microcantilever beam. The most common testing methodology introduces target molecules to the cantilever where they are absorbed by bioreceptors. This adsorption results in an increase in mass on the cantilever tip generating mechanical stress that causes the cantilever to deflect. The success of this approach stems from allowing label-free mass detection of the molecules of interest. The typical detection method relies on the reflection of laser light off the canitilever tip to a photosensitive detector that produces an electrical signal proportional to lever deflection. Moreover, the size of these devices makes it possible to fabricate high-density parallel sensors for high-throughput analysis. This method affords high sensitivity (in the sub-nm deflection range), but requires the optical alignment of space consuming setups, hence severely limiting the exploitation of such technology in viable lab-on-chip architectures. Other common

methods exploit direct transduction of the cantilever deflection into an electrical signal through piezoresistive or piezoelectric levers. The latter approaches have the advantage of eliminating alignment steps, but often suffer from sensitivity concerns [9].

A prominent field of study in biosensor development, and the primary focus of this research, is the study of electrochemical behavior in which electric signatures like resistance, reactance, relaxation times, and diffusion effects provide valuable insight into the fluids contents and behavior under the influence of mediated and unmediated electron transfer [10]. In biosensing, relevant electrical properties that characterize biological phenomena are typically electrochemical in nature and occur in relatively close proximity to the electrode surface. As such, electrode geometry, material, and surface modification will determine the sensing ability of the device. Hence, the distinct advantage of existing electrode designs that are easily incorporated into LOC technologies indicates significant promise in the field of electrochemical sensing. Typically in bioelectrochemistry, the reaction under investigation would generate a measurable current (*amperometric*), a measurable potential or charge accumulation (*potentiometric*), measurably alter the conductive properties of a medium (*conductometric*) between electrodes, or induce changes in impedance between two electrodes (*impedimeteric)* [11].

In amperometric devices, the current generated by an analyte when it interacts with an electrode surface under an excitation potential is measured. Typically, a three electrode configuration consisting of a working electrode, a reference electrode, and an auxiliary electrode is employed. The working electrode is ideally polarized and highly conductive to gather relevant information regarding electrochemical phenomena inherent to the electrode. An appropriate potential is applied to the working electrode with respect to the

reference electrode and the generated current between the working electrode and the auxiliary electrode is measured [12]. The auxiliary electrode captures impedimeteric data in the solution and must be located in close proximity to the working and reference electrode enabling ease of miniaturization.

Potentiometric sensors detect the potential charge accumulation at the working electrode in comparison to the reference electrode in an equilibrium state where no current flows between them. These devices are governed by the Nernst equation, given as (1) [13]:

$$E_{cell} = E^{O}_{cell} - \frac{RT}{nF} lnQ \quad (1)$$

, where E_{cell} represents the cell potential at zero current, E^{O}_{cell} is the constant potential contribution to the cell, R is 8.3145 J/Kmol, T is the absolute temperature in degrees Kelvin, n the charge number of total reaction at the electrode, F is 96485.3329 C/mol, and Q is the ratio of ion concentration at the anode to the cathode. The relationship between analyte concentration and potential is suitable for measuring low analyte concentrations in minute sample volumes making potentiometric technology a viable means of bio agent detection.

Conductometric devices use a two-electrode configuration to measure the ability of an analyte to conduct electrical current between them. The addition of an analyte suspended in an electrolytic solution perpendicular to a planar electrode surface, enables the conductivity of the target to be measured. Sheppard et al. reported the relevance of electrode geometry to conductometric device function reasoning that device sensitivity increased with electrode surface area giving way to the application of an interdigitated electrode (IDE) in electrochemical conductometric sensors [14]. These devices offer a

number of advantages most significantly their ease of manufacturing and their detection methodology for a number of analytes.

A common corollary of conductometric devices is impedimeteric sensors. Impedimetric biosensors enable the observation of material properties and reactions within an electrochemical cell that can alter the systems conductivity/resistivity or capacitivity at the electrode/analyte interface. Unlike conductometric technologies, impedimeteric devices do not require a conductive analyte solution provided the data collection method has sufficient range to capture low and high level variations of resistivity/conductivity within the system. The application of an excitation voltage to an impedimeteric electrochemical cell generates immediate resistive and/or capacitive responses at the electrode/analyte interface that can be readily monitored with basic technologies. As a result, the devices are ideal in situations where rapid detection and sensing agility are critical metrics of performance. Thus, an impedimeteric biosensing modality is selected for further research in this study.

1.3 Electrochemical Glucose Detection- State of the Art

Diabetes mellitus or simply diabetes is a chronic disease that manifests when the pancreas either does not produce insulin (*Type 1*) or fails to process sufficient insulin (*Type 2*) to convert glucose into energy [15]. Lack of insulin production and efficacy results in elevated glucose levels in the bloodstream, a condition commonly referred to as hyperglycemia. As a result diabetes produces an onslaught of general health complications including cardiovascular disease, blindness, renal failure, extremity amputation, and death. According to the International Diabetes Federation, 415 million people worldwide are

afflicted with diabetes, and an estimated 642 million people will be diagnosed in 2040 [16]. That is to say, in 2040, one out of every ten people in the world will contract diabetes. As a result of this epidemic, diabetic research is an ever-expanding field with a particular emphasis on various treatment methodologies and hyperglycemic monitoring modes in the hopes of limiting diabetic effects and improving patients' overall quality of life.

Current diabetes monitoring techniques are effective, but they require patients to take measurements several times throughout the day in which a finger prick is necessary. Furthermore, these readings can only be collected when the patient is awake imposing interruptions in sleep patterns and often, more critically, radical shifts in glucose levels throughout the night. A continuous glucose monitoring (CGM) system consists of three parts; a sensor, a transmitter, and a receiver. CGM not only eliminates the requirement of excessive blood collection, but also provides valuable glucose trend data and life-saving insulin delivery in off-peak hours. While CGM systems are currently available to consumers, sensor life is typically limited to seven days or less and the systems can be costly and inaccurate with up to a 15% variation when compared to current "finger-stick" methods [17]. To date, a stable, cost effective, and accurate means of continuous glucose monitoring at the patient level has not been identified presenting a significant research opportunity. The development of the first biosensor, an enzymatic, amperometric glucose sensor, by Clark and Lyons in 1962 generated a tremendous effort to improve and develop the technology that continues today. Primary efforts are focused on detection stability as biological agents like GOx are by nature sensitive to their physio-chemical environment necessitating careful consideration with regard to storing and usage and eliminating the possibility of continuous glucose monitoring. In addition, enzyme immobilization on a bare

electrode can be complicated making scalable production and quality difficult to achieve.

In recent years, the demand for glucose monitoring techniques is rivaled only by the expansive increase of proposed exploratory devices. The desire for an effective reliable means of glucose monitoring could greatly increase the quality of life for a substantial percentage of the world's population. As the topic matures, the research community has divided glucose sensing technology into two primary categories: sensing based on existing enzymatic technologies, and enzyme-free detection methods with the majority of emphasis placed on enzymatic sensing. Current glucose monitoring techniques employ a test strip treated with glucose oxidase (GOx). Glucose ($C_6H_{12}O_6$), present in a droplet of blood, reacts with the enzyme and oxidizes to form gluconic acid ($C_6H_{12}O_7$) and peroxide (H_2O_2) as given in (2) [18].

$$C_6H_{12}O_6 + H_2O + O_2 \xrightarrow{GOx} C_6H_{12}O_7 + H_2O_2 \quad (2)$$

Although quality improvements in enzyme based detection are still being made, there are a number of complications associated with enzymatic glucose sensors such as difficult enzyme immobilization procedures and environmental sensitivity [19]. Moreover, the biological nature of these devices equates to a short shelf life, high fabrication costs and single use limitations. As the number of diabetic cases continues to rise, researchers have shifted their focus to a possible solution in non-enzymatic glucose detection (NEG) to overcome the limitations of the current technology. Referred to as the 4th generation of glucose sensors, NEG technology employs the direct interface between the electrode and target molecule without the aid of an unstable biological interface [20]. This enables the concept of real time monitoring and long term stability.

Unlike their enzymatic predecessors, NEG sensors rely on modifiers at the surface

of the electrode as an electrocatalyst of glucose oxidation [21]. Numerous efforts using a vast array of porous layers [22, 23, 24, 25] graphene [26, 27], nanotubes [28], oxides [29, 30, 31, 32], nanoparticles [33, 34, 35] and alloys [36] have been explored as potential sensing mediums in primarily amperometric and potentiometric studies. The complex nature of preparation for nanoparticles and thin film based mediators have been rigorously investigated in recent years even to the point of their necessity with numerous experiments based on data obtained from bare metal electrodes devoid of any modifiers [35]. Although the majority of these works are effective means of characterizing specific analytes, the electrochemical kinetics and mechanisms of NEG technology remain ambiguous with limited scientific exploration.

Electrochemical impedance spectroscopy (EIS) is a potential means of transduction for these devices that addresses this issue. In EIS, a small potential is applied to an electrochemical cell over a wide range of frequencies in the Hz to kHz range, and the impedimeteric response is captured for analysis [37]. The EIS spectrum yields significant impedance and admittance values relevant to the electrode and analyte such as conductivity, dielectric constant, and charge mobility, or the system's behavior at the electrolyte/electrode interface [38]. For the purpose of glucose measurement, EIS is based on the evaluation of the change of charge transfer resistance, R_{ct}, as a function of glucose concentration [39] and [40]. The data, typically presented via Nyquist or Bode plots, is indicative of the electrode/electrolyte behavior as well as the chemical surface kinetics. These behaviors alter the R_{ct}, and thus can then be levied against their analogous electronic counterparts in an electrical equivalent circuit (EEC) to generate an idea of the interaction of any analyte at the electrode interface. More succinctly, biodetection methods using EIS

are not limited to glucose monitoring provided changes in electrochemistry generate measurable changes in impedimeteric response.

EIS can be configured to monitor molecular phenomena in an analyte at a fixed frequency over long periods of time. This facilitates high precision continuous monitoring of glucose levels eliminating the need for an EEC. However, optimal experimental values including complex impedance and voltage perturbation levels are still required to identify an optimal frequency to conduct a fixed frequency analysis.

In this research, a NEG device is fabricated, characterized and employed as a means of real time monitoring of glucose concentration change using EIS. A bare gold planar electrode in a band/gap interdigitated configuration is used. Conventional data acquisition techniques over a broad frequency range are conducted in order to obtain a fixed frequency spectrum for real time measurement of various glucose concentrations. In addition, critical aspects of data acquisition, processing and linearization are also examined.

II.ELECTROCHEMICAL IMPEDANCE SPECTROSCOPY

Electrochemical impedance spectroscopy (EIS) is a promising detection method for a variety of viral, bacterial, and chemical agents in biological environments capable of capturing biological reaction behavior in close proximity to an electrode surface [41]. In EIS, the output signal (current) generated by an applied AC potential at a range of frequencies is collected and approximated to an equivalent circuit to extract relevant details in regard to the analyte. Founded in the 1880's by Oliver Heaviside, EIS is based on two distinct elements: impedance, and admittance [42]. These responses are a product of the reactant response that arises from inductive, capacitive, and resistive effects of the target analyte. EIS is highly regarded as a viable detection method for a number of biological evaluations including the presence of food-borne bacteria [43], DNA hybridization [44], listeria [45], protein markers [46], as well as glucose concentrations [47].

2.1 Definition of Impedance

The rapid and accurate measurement of electrochemical phenomena is of considerable importance for a range of studies. In electrical circuit theory the concept of resistance abides by Ohm's Law. While this is an effective means of analysis for ideal resistors, real world applications demonstrate more complex behavior demanding an explicative resistive element called impedance. Impedance, defined as the effective resistance of an electric circuit or component to alternating current, arising from the combined effects of ohmic resistance and reactance generated from resistors, capacitors and inductors that impede the flow of electrons [38]. In a purely resistive circuit, voltage and current are said to be in phase with each other. That is, the sinusoidal voltage and

current waves are synchronized over a period of 2π as shown in Figure (1a). However specific circuit elements like capacitors and inductors shift the current response to either lead or lag the voltage perturbation. These responses are termed capacitive (3) and inductive (4) reactance respectively.

$$X_c = \frac{1}{j\omega C} \tag{3}$$

$$\mathrm{X_L} = j\omega L \tag{4}$$

, where j is $\sqrt{-1}$, ω is the angular frequency ($2\pi f$), C is capacitance in farads and L is inductance in henrys.

Capacitive circuit elements generate a negative phase shift angle of as current leads voltage while purely inductive elements generate positive phase angles as shown in Figure 1 (b) and (c) respectively. Inductive behavior in an electrochemical cell is rare and often contributed to experimental errors, such as electrode contamination or fouling, faulty equipment, or improper use [48]. Electrochemical impedance is measured by applying an AC potential (excitation voltage) and measuring the resultant current through the electrochemical cell. The sinusoidal current response to the small applied potential will occur at the same frequency only shifted in phase. This phase shift enables the measurement of electrochemical impedance.

Impedance, henceforth denoted as Z, is the ratio of the sine-wave amplitude of a polarization potential of constant value called the excitation signal, and the sinusoidal current response of the same frequency that differs in amplitude and phase. Akin to Ohm's Law, Z is derived by:

$$Z = \frac{E_o \sin(\omega t)}{I_O \sin(\omega t + \theta)} \tag{5}$$

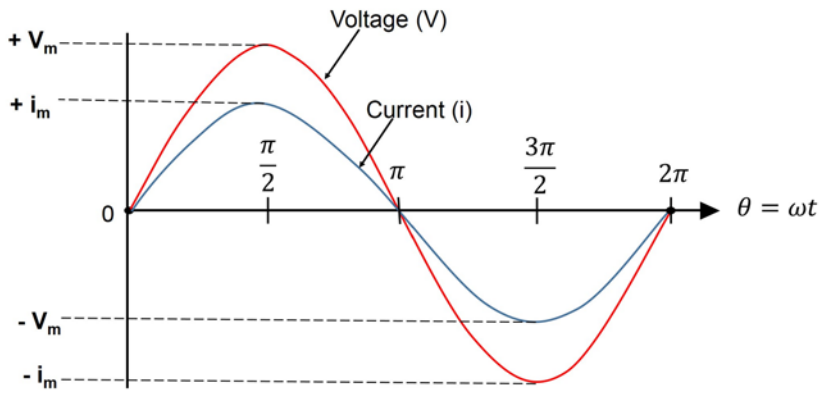

(a)

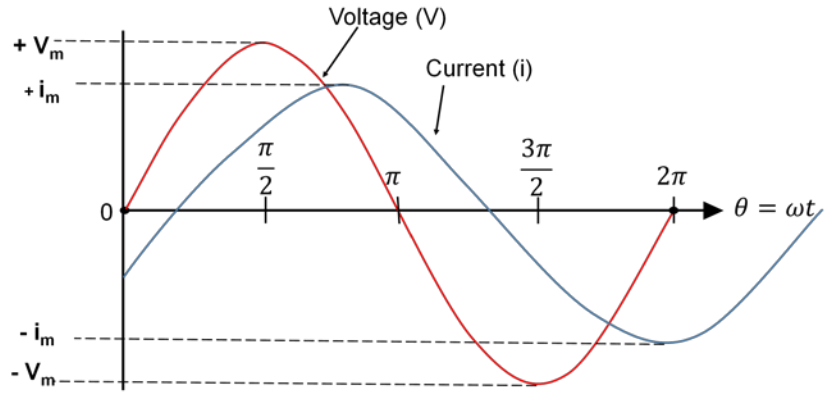

(b)

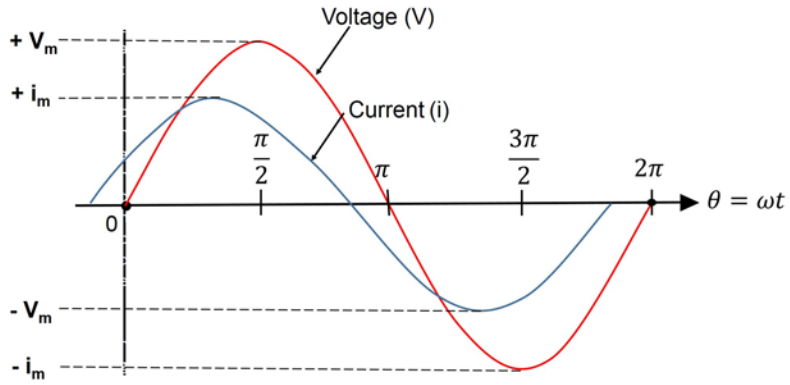

(c)

Figure 1: The sinusodial behavior between current and voltage at a particular excitation potential. (a) represents no phase change between voltage and current or a purely resistive element. (b) illustrates capacitive behavior in which voltage lags current. (c) displays inductive behavior in which voltage leads current.

, where E_0 is the amplitude of the excitation signal, ω is the radial frequency ($2\pi f$), t is time, I_O is current amplitude, and θ is the phase angle.

2.2 Data Representation in EIS

The impedance spectra can be analyzed in reference to either the time or frequency domains. Signals in the time domain are represented as amplitude with respect to a timing element. Frequency domain analysis represents signal amplitude with respect to frequency. EIS data is displayed as either a vector or a complex quantity as shown in Figure 2. Vectors are defined by both the magnitude of the signal, and its corresponding phase angle. Contrarily complex impedance data is represented on a complex plane with the real element on the x-axis and the imaginary component on the y-axis. It is important to note that both representations of the signal are computationally equivalent with each technique possessing distinct advantages depending upon the application and analysis technique. The two most common representations are the Nyquist and Bode plots.

In a Nyquist plot, the overall cell impedance is represented by its real and imaginary components often denoted Z' and Z" respectively. Impedance is represented as a vector quantity of length |Z| with phase angle between |Z| and the x-axis as shown in Figure 3. Often, the shape of the plot is used to analyze the physical behavior within an electrochemical cell in the time domain with geometric characteristics corresponding to certain electrochemical behaviors. For example, the semicircle in Figure 3 is indicative of a single time constant or rather one iteration of a kinetic event spanning the frequency spectrum. With the proper analysis, the Nyquist plot is invaluable for determining electrochemical behavior within a cell. However, a major deficiency is the lack of relevant

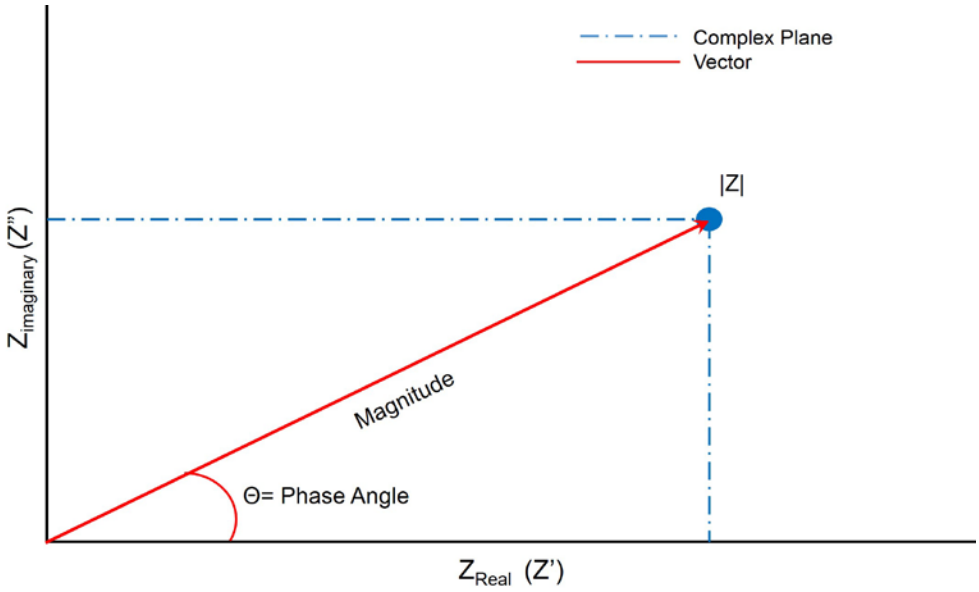

Figure 2: The complex and vector quantities of impedance, |Z| are shown with the complex value illustrated as a blue dot and the vector quantity as a red arrow. Note the angle between the x-axis and vector quantity as phase angle.

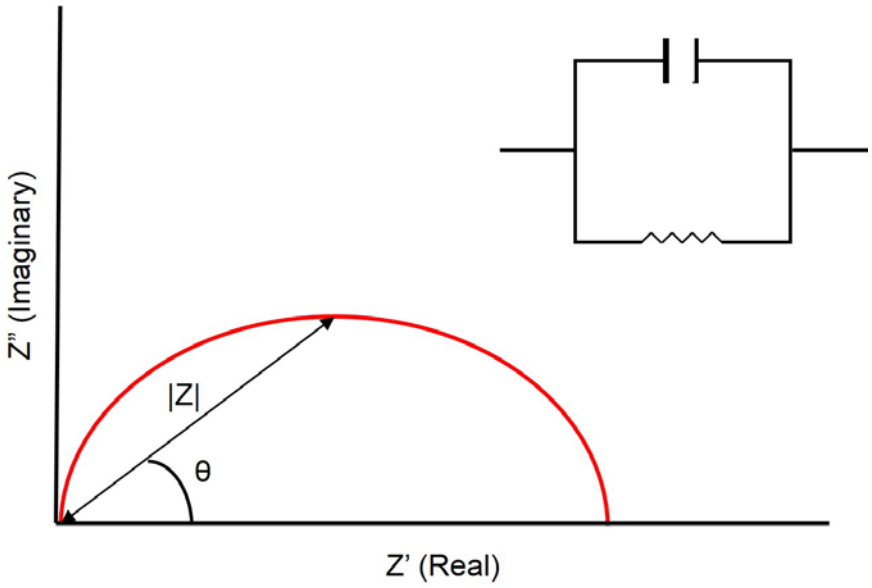

Figure 3: The Nyquist plot exhibiting the behavior of the capacitive EEC schematic as well as the impedance vector |Z| and phase angle is shown.

frequency data for each point of measurement in the spectrum. A Bode Plot is used to model frequency responses within the electrochemical cell. Bode plots are a combination of both |Z| values and phase responses throughout the frequency spectrum as shown in Figure 4. Unlike Nyquist plots, Bode representations aid in identifying relevant, frequency-driven data for individual charge transfer mechanisms.

2.3 Modeling Data

The Nyquist and Bode plots shown in Figures 3 and 4 are manifestations of the circuit schematics at the inset in the top right hand corner, a capacitor in parallel with a resistor. Generally, EIS data is characterized using an electrical equivalent circuit model (EEC) by which the often complex behavior of electrochemical cells is categorized into an analogous electronic circuit. The proper arrangement of passive electric circuit components can mimic the behavior of the electrochemical system. Thus, the complex behavior of biologic systems can be discretely quantified and used to establish a sensing methodology. EIS techniques rely on one of two different models: physical or empirical. In an empirical model, the equivalent circuit devices are not assigned to the behavior of the system but rather are implemented to provide the best possible fit of impedimetric data versus measured impedance of the cell. Empirical models are constructed by subtracting known impedances from the electrochemical cell. If the known impedance simplifies the cell, the component is added to the equivalent circuit until the model best matches the measured impedance values. In a physical model, each circuit component corresponds to a physical electrochemical event within the cell. Taking into account the physical characteristics, users assemble the model based upon the shape of the impedance spectra employing a

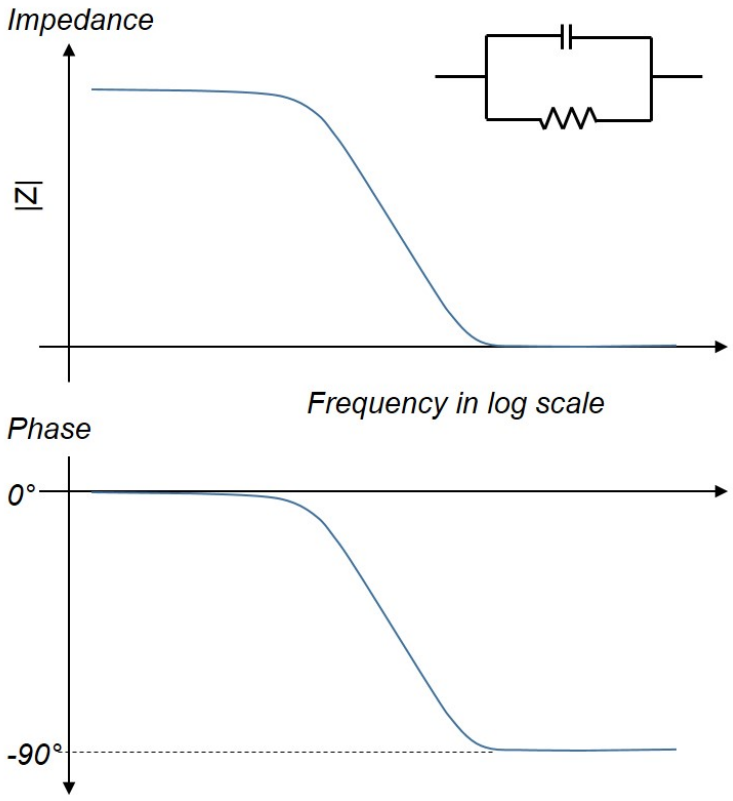

Figure 4: A Bode plot exhibiting the behavior of the electrical equivalency circuit with one time constant shown in the inset. The impedance response and phase response.

"simpler is better" approach. In this way, electrochemical phenomena can be adequately explained.

2.4 Randles Cell

A common interpretation of the impedance spectra is the Randles cell. Shown in Figure 5 (a), the Randles cell consists of an active solution resistance (R_{sol}) in series with a parallel combination of double layer capacitance (C_{dl}) and the series combination of charge transfer resistance (R_{ct}) with a Warburg impedance (Z_w) element. The frequency response of the Randles cell is described by two electrochemical events. The first characterizes the diffusion response, while the second is kinetic charge transfer. At low frequencies, the model illustrates Warburg diffusion denoted by the straight line at a 45˚ angle until sufficient frequency enables a kinetic charge transfer reaction as shown in Figure 5 (b). Analogous to elements within many physical systems, the Randles cell often serves as a baseline when modeling electrolytic behavior of biological systems [49].

2.5 Electrochemical Circuit Elements

Analogous to resistors, capacitors, and inductors, elements of electrochemical cells can impede the flow of electrons and generate changes in the response current. Electrode kinetics, interfacial chemistry, and diffusion reactions directly impact an electrochemical system. The following circuit elements are relevant to this research and are by no means a comprehensive list. However, an exhaustive list of electrochemical elements is demonstrated by Yuan et al. [49].

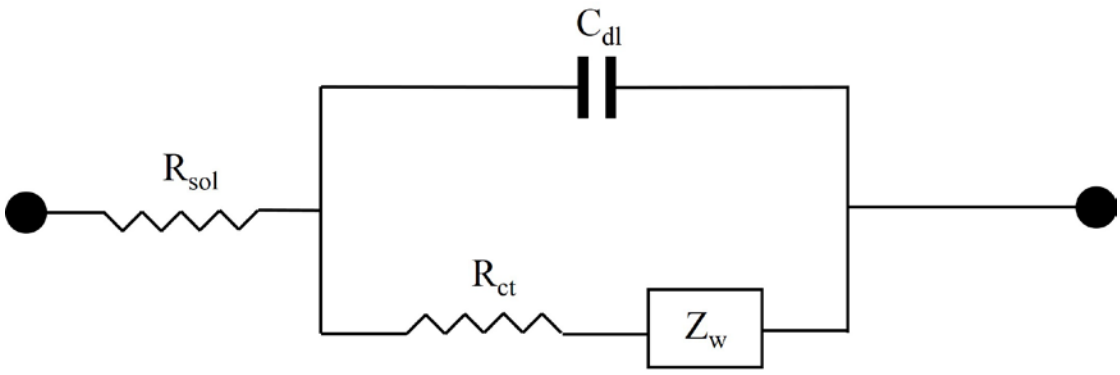

(a)

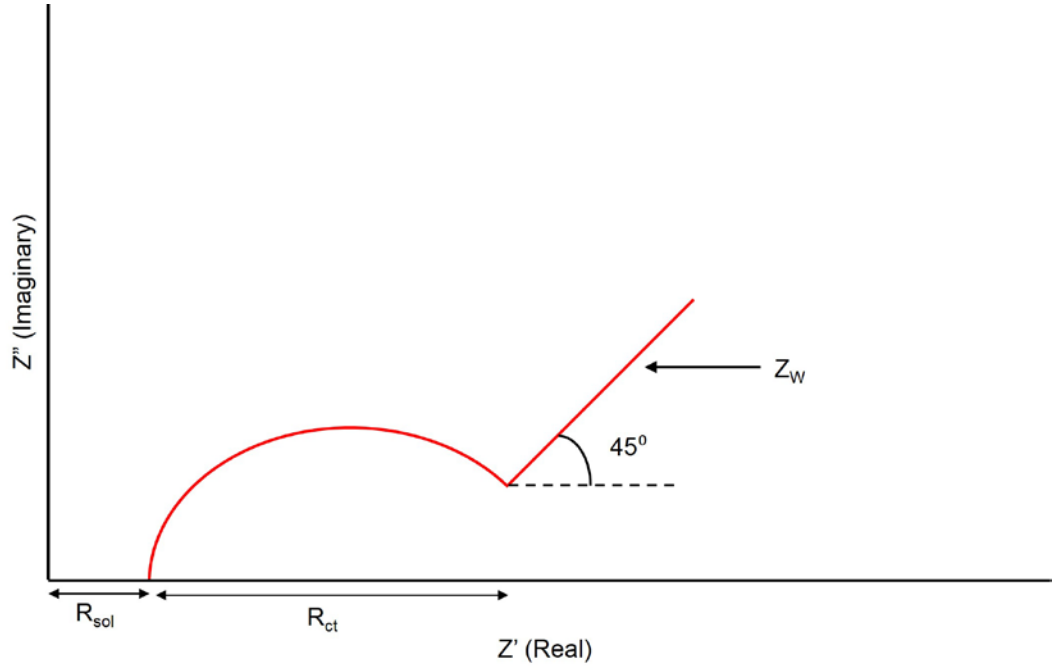

(b)

Figure 5: The Randles Cell with an (a) electrical equivalency circuit and (b) the impedimetric behavior of the Randles Cell as plotted on a Nyquist Diagram.

2.5.1 Double Layer Capacitance and Constant Phase Element

An electrical double layer exists on the interface between an electrode and its surrounding electrolyte. This double layer is formed as ions from the solution adsorb onto the electrode surface. A negatively charged electrode will repel anions while simultaneously attracting cations to its surface thus polarizing the electrode/electrolyte interface. As shown in Figure 6, the charged electrode is separated from the charged ions by an insulating space or molecular dielectric called the Helmholtz plane. The distance between the upper and lower boundaries of the Helmholtz plane is in the order of angstroms.

Regardless, charges separated by an insulator form a capacitor, thus a bare metal immersed in an electrolyte will behave like a capacitor. The value of the double layer capacitance depends on many variables such as electrode potential, temperature, ionic concentrations, types of ions, oxide layers, electrode roughness, impurity adsorption, etc. Thus, electronic characteristics at the electrode/electrolyte interface do not behave as strict capacitors. Rather, a constant phase element (CPE) is introduced. A CPE is an empirical pseudo-capacitor that mimics imperfect capacitance and is often used to resolve unknown phenomena within an electrochemical cell. Constant phase impedance can be calculated as:

$$Z_{CPE} = \frac{1}{(j\omega)^{\alpha} C_0} \tag{6}$$

, where, C_0 is the capacitance and α is an exponent ≤ 1. In a true capacitor, α is equal to 1. In most bioelectronics, ideal capacitance is not possible, hence CPE offers a suitable alternative for fitting impedimeteric data.

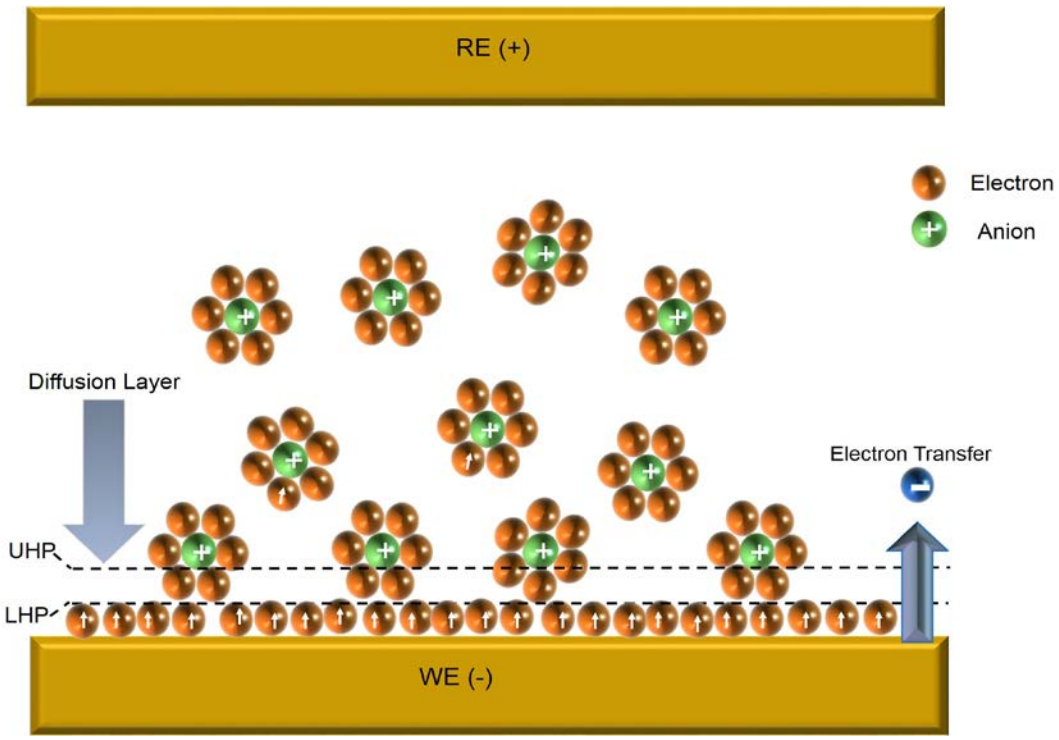

Figure 6: A schematic diagram of charge transfer from working electrode (WE) to reference electrode (RE) via electrolytic carriers. Arrows represent polarization effects of an applied potential on electrons.

2.5.2 Charge Transfer Resistance

Charge transfer resistance (R_{ct}) is resistance of electron transfer from the electrode surface through the liquid solution containing the target analyte. Like any substance, the transfer of these electrons must be associated with a certain degree of resistance given in ohms (Ω). This ohmic resistance is driven by a kinetically controlled electrochemical reaction called a reduction oxidation reaction (redox) given as,

$$R_{ed} \leftrightarrow Ox^{+} + ne^{-} \tag{7}$$

In electrochemical redox reactions, ions enter the electrode and the electrode diffuses into the electrolyte thus transferring charge. In this case the electrode is the reductant and the electrolyte is the oxidant. The reaction takes place only after electrons overcome a resistance between the electrode and the electrolyte. This transfer resistance is driven by a number of environmental conditions including but not limited to temperature, atmospheric pressure, excitation voltage, and reactant concentration in bulk solution.

2.5.3 Solution Resistance

Another significant resistance vale in EIS is electrolytic solution resistance (R_{sol}). An excitation voltage, applied to an electrode in an electrochemical cell, generates current flow. The efficiency of current flow is influenced by the electrolytic media. Ions in solution serve as electron carries through an electrolyte from anode to cathode. The more ions present in the solution, the lower the impedance value. Ionic concentration is not the only limiting factor. In an area of constrained geometry carrying uniform current, resistance is defined by the formula:

$$R = \rho \frac{l}{A} \tag{8}$$

, where ρ is solution resistivity, l is length of the cell, and A is the area of the cell. However, determining a linear current flow path and geometry is impractical due to fringing effects, electrode surface topography, and other amperometric phenomena in the electrolyte. Consequently, the value of R_{sol} through the cell is obtained by fitting impedance data to an EEC model and generating simulated R_{sol} results.

2.5.4 Diffusion (Warburg Impedance)

Diffusion effects can also contribute to system impedance by generating a frequency dependent element known as Warburg impedance (Z_w). In an electrochemical cell, there is a finite distance between sensing electrodes, and reactants in solution. The analyte travels this distance to drive a chemical reaction to completion thus enabling a sensing modality. For example, at low frequencies target analytes travel long distances to contact the electrode generating large Z_w values while, at high frequencies the effects of Z_w are negligible. The 45˚ linear portion in Figure 5 describes the effects of diffusion. As Z_w decreases with growing frequency, total impedance |Z| is decreasing linearly until a sufficient frequency generates kinetic charge transfer as evidenced by the hemispherical curve. There are two types of Warburg responses dependent upon the type of electrochemical cell, finite and infinite. Infinite Warburg refers to systems with diffusion layers with infinite thickness in regards to the scale of the system in question. In the case of most sensing technologies, this is not the case. In instances where the diffusion layer is bounded, for example, by the closed dimensions of a fluidic channel that holds an analyte, the finite Warburg element is used.

III. EXPERIMENTAL METHODOLOGY

3.1 Design

The electrochemical reaction between the electrode and experimental solution occurs either at the electrode surface or in close proximity. Thus, the electrodes themselves are paramount to the performance of the device. Careful consideration is given to both the electrode material as well as its substrate. A standard borosilicate microscope slide (Fisher Scientific 12-544-1 Pittsburgh, PA) is chosen as a substrate as it is readily available, inexpensive, and are easily incorporated into other LOC designs.

The interdigitated planar electrode (IDE) design shown in Figure 7 (a) is chosen and arranged longitudinally on the slide. Each IDE array measured five millimeters long by 20 mm wide with each band in the arrays measuring 6 mm x 50 µm with a 50 µm gap between each band. Each substrate contained a total of four arrays with one (E1), three (E2), five (E3), and seven (E4) electrode pairs arranged in a band/gap configuration.

Biomimetic flow of the solution to simulate capillary blood flow is an important consideration to the design of the device. While conventional glucose screens rely on a static droplet analysis continuous glucose monitoring suggests a steady flow of analyte. To simulate this behavior the microfluidic channel shown in Figure 7 (b) is incorporated to serve as a carrier for the sample solution to each electrode interface. The microfluidic is designed with a 1:1 ratio of 100 µm spanning the entire length of the electrode array. Five inlets are incorporated to enable the introduction of varying analyte concentrations in rapid succession as well as a single outlet for future connections.

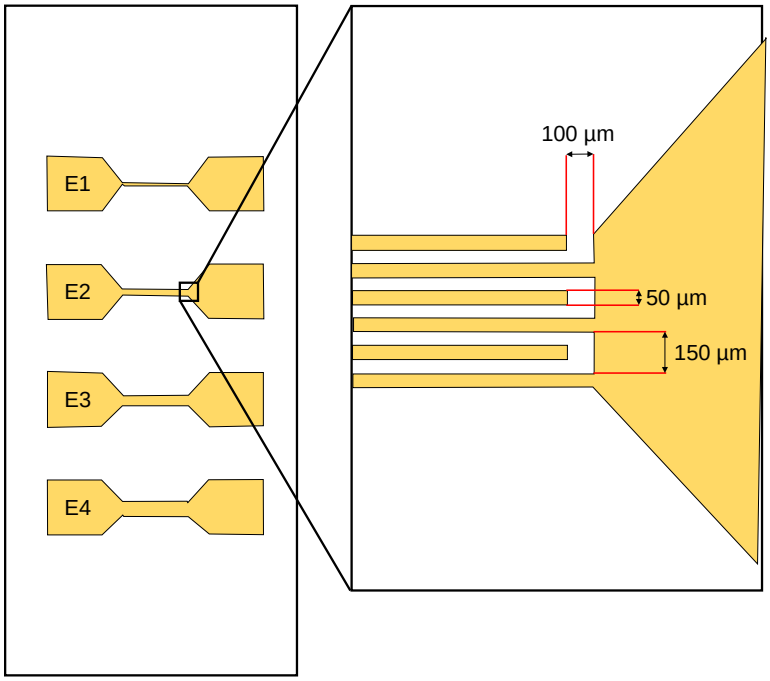

(a)

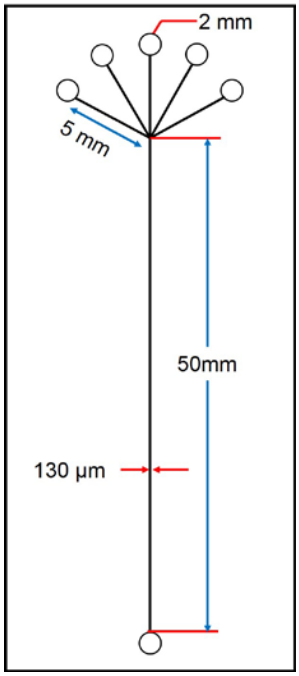

(b)

Figure 7: (a) The electrode array design with band/gap dimensions. E1 has one pair, E2 has 3 pairs, E3 has 5 pairs, and E4 has 7 pairs of interdigitated electrodes. (b) The microfluidic channel design with a 100 µm x100 µm channel width beginning with five inlets and terminating with one outlet.

3.2 Fabrication

3.2.1 Electrode Patterning

The interdigitated electrode arrays are fabricated on a glass substrate. The process is divided into four steps: cleaning, photolithography, metallization, and liftoff. The process flow shown in Figure 8 (a-e) and described below is conducted in a cleanroom.

A cleaning process is crucial to ensure adequate adhesion of photoresist and metallization layers. Any contamination of the surface could later result in voids or irregularities in the electrode surface. The process begins by loading each slide into a spin coater and subjecting it to a standard solvent clean with acetone, methanol, and isopropyl alcohol respectively at 3000 RPM to remove any particulates or residues present from the manufacturer. The slide is rinsed in DI water, dried and dehydrated in a convection oven at 100°C for 10 minutes. Following the solvent clean, the samples are submerged in Nanostrip (KMG Chemicals Fort Worth, TX), heated to 60°C for a period of 15 minutes to remove any remaining organic and inorganic contaminates. The slide is then rinsed in running DI water for 2 minutes, dried with nitrogen, and dehydrated in a convection oven for 10 minutes (Figure 8(a)). Prior to depositing photoresist, hexamethyldisilizane (HMDS) is applied to the glass at 3000RPM for 30 sec to improve photoresist adhesion. The substrate is placed on a hot plate set to 125°C for 3 minutes to evaporate excess solvent remaining from HMDS. AZ 5214E (Microchemicals GmbH, Ulm, Germany) photoresist is spun on the glass at an initial speed of 500 RPM for 10 seconds followed by 3500 RPM for 45 seconds to achieve a thickness of 1.4 µm followed by a soft-bake at 125°C. Upon reaching ambient temperature, the slide is loaded into a UV aligner (Carl Suss MJB4 Garching, Germany) for an exposure dose of 78 mJ/cm^2 (Figure 8 (b)).

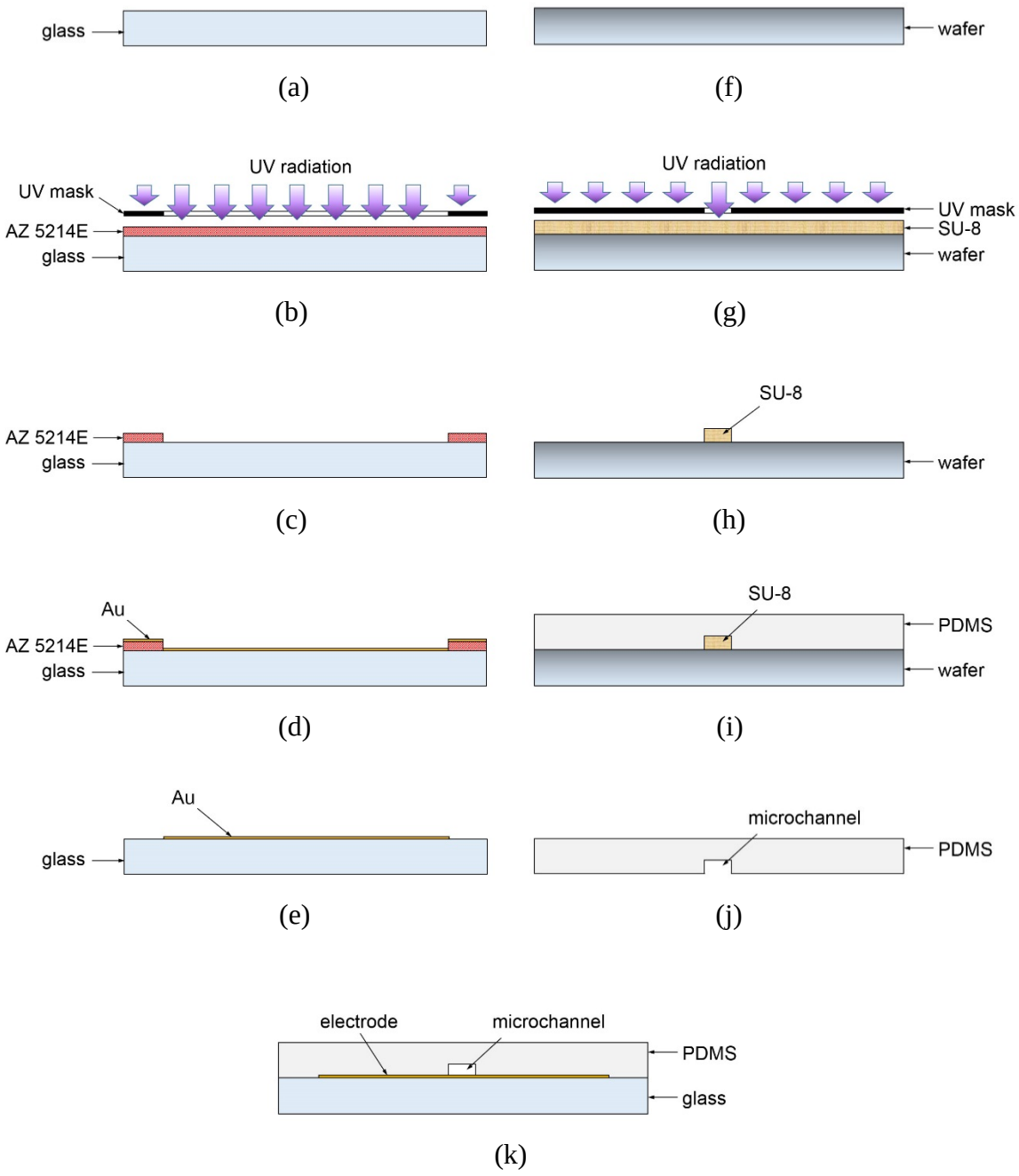

Figure 8: A schematic of the device fabrication process. (a) A clean borosilicate glas slide. (b) Photoresist Exposure (c) Photoresist development.(d) Metal deposition (e) Photoresist liftoff. (f) Clean Si wafer (g) SU8 exposure (h) SU8 development (i) PDMS application over moldmaster. (j) Removal of microfluidic channel from mold master. (k) Bonding of PDMS microchannel with glass substrate via O_2 plasma.

The photolithography process is completed by submerging the substrates in MIF 300 (AZ Electronics Materials, Somerville, NJ) to develop the exposed photoresist. The substrate is rinsed and inspected via microscope. Photoresist remnants within the defined electrode geometry are removed from the samples using oxygen plasma asher at approximately 80 watts and 15 sccm for a period of 10 seconds (Figure 8 (c)). Upon satisfactory inspection, the slides is dehydrated in a convection oven at 90°C before metallization.

Gold is selected for the electrode due to its reduced oxidation potential at neutral pHs thus limiting signal degradation due to fouling [24]. Gold is deposited on the entire substrate via electron beam evaporation (Figure 8 (d)). Six sample substrates are loaded onto the carrier of the e-beam evaporator (Evovac PVD, Angstrom Engineering, Kitchener, Ontario, Canada) and the chamber is pumped down to 20×10^{-9} Torr. An adhesive layer 5 nm thick of titanium is applied at a rate of 1.5 Å/sec followed immediately by the 100 nm functional layer of gold. The chamber is vented and the metal-coated substrates are removed from the chamber.

Following metal deposition, the substrate is submerged in acetone for 2 minutes. This soaking period begins to dissolve the photoresist leaving only the metal electrode on the glass substrate. The substrates is agitated in an intermittent ultrasonic bath until no photoresist remained (Figure 8 (e)). The electrodes are rinsed in DI water, dried with N_2 and inspected with an optical microscope to confirm the correct electrode structure and identify any defects.

The final step in the fabrication of the electrodes is a metrological inspection to ensure designed dimensions are represented in the fabricated electrodes. Using a Nikon

MM-800 Measurescope (Nikon Metrology Inc., Tokyo, Japan) the relative electrode dimensions of 3 separate electrode sets are measured with the results shown in Table 3.1. Figure 9 shows the gold electrodes on the glass substrate.

Table 3.1: The dimenisons of individual electrode pairs taken from 3 electrode sets that are averaged and compared to the design intent in Figure 7 (a).

	Design (Figure 7 (a))	Fabricated
Electrode Band	50 µm	50.06 ± 0.63 µm
Electrode Gap	50 µm	50.64 ± 0.82 µm
Band/Gap	150 µm	150.725 ± 0.38 µm

3.2.2 Microfluidic Channel

The microfluidic channel began with the fabrication of a mold master constructed in SU-8 2050 polymer photoresist on a 100mm (100) Si wafer. SU-8 2000 is spun at 4500 RPM as a 2 µm adhesive layer between thick SU-8 2050 photoresist and the Si wafer and soft-baked in two stages: the first at 65°C for 5 minutes followed by 95°C for 2.5 minutes on a completely level work surface. A UV exposure of 80 mJ/cm^2 is applied to wafer without a UV mask to crosslink and solidify the adhesive layer. The wafer is returned to the spin coater where SU-8 2050 is spin-coated at 1200 RPM yielding a film of approximately 130 µm. Edge bead removal is accomplished chemically by applying a steady stream of SU8 developer along the edge of the wafer at 100 RPM followed by a ramped soft bake of 5 minutes at 65°C and 30 minutes at 95°C. Following the soft bake, the wafer is loaded into the UV aligner and exposed to a 265 mJ/cm^2 dose (Figure 8 (g)). A post exposure bake of 5 minutes at 65°C and 12 minutes at 95°C followed by submersion

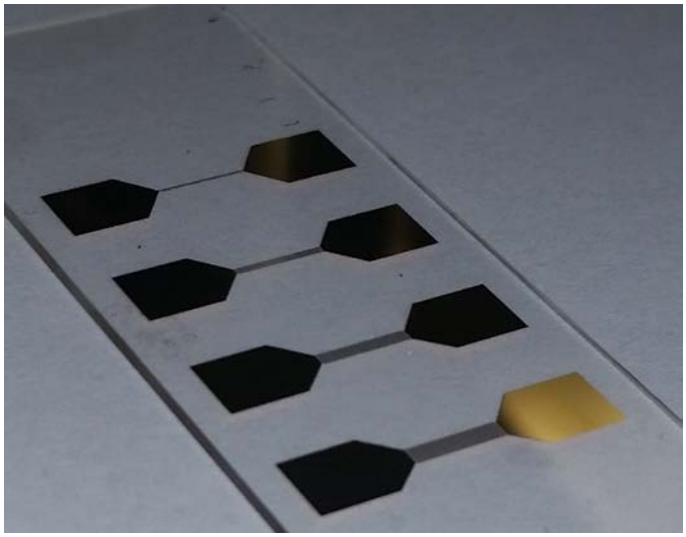

Figure 9: The fabricated gold electrode set on a glass substrate.

development in SU-8 developer (MicroChem Corp, Westborough, MA) to reveal the final structure, a negative of the microfluidic channel as shown in Figure 8 (h). The 130 µm thick SU-8 mold master is shown in Figure 10.

The microfluidic channel is fabricated in polydimethylsiloxane (PDMS) (Sylgard 184 Elastomer, Dow Corning, Midland, Mi). PDMS is widely used silicone-based polymers in microfluidics [50]. The ease of fabrication, low cost, biocompatibility, elastomeric property, and optical transparency are attractive reasons for its wide usage in rapid prototyping of biomedical devices. The process begins by placing the mold master in a circular reservoir large enough to encompass the entire wafer. The PDMS is mixed as per the manufacturer's instructions in a 10:1 ratio of polymer resin to hardener and applied over the entire wafer in the reservoir. The mold master PDMS matrix is placed in a vacuum desiccator to remove air bubbles in the PDMS. When no entrapped air remained at the sample surface, it is desiccated a final time to ensure no air is present in the elastomer and the assembly is placed on a 90°C hotplate to solidify the elastomer for a period of 15 minutes (Figure 8 (i)). At room temperature, the cured PDMS is cut along the edges of the microfluidic structure and peeled away from the mold master resulting in the microfluidic channel shown in Figure 8 (j). A petri dish lid is placed over the top of a sample electrode and the electrode access ports are cut.

To ensure the microchannel dimensions, a sacrificial microchannel is fabricated and cleaved at different locations along the fluidic channel and measured. As shown in Figure 11, the dimensions of the channel are 102 µm wide and 130 µm tall.

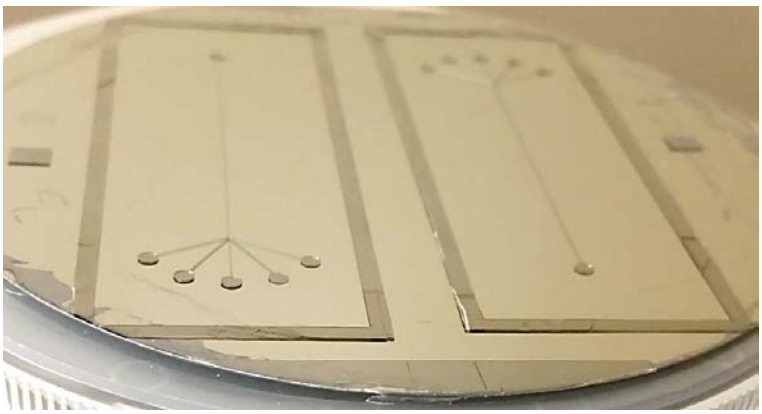

Figure 10: The microfluidic mold master fabricated in SU8 photoresist. By flipping the wafer and blocking the electrode design of the UV mask, two mold masters are generated on the same wafer.

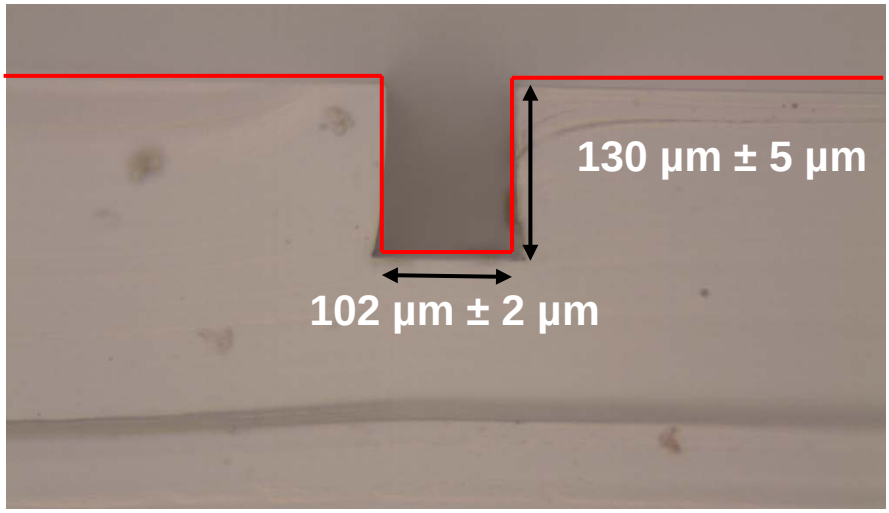

Figure 11: A cross-section of the microfluidic channel with the average height and width.

3.2.3 Assembly

The final step in device fabrication is the assembly of the PDMS microfluidic channel and the glass substrate with Gold electrodes. An oxygen plasma bond is used to ensure a uniform permanent seal between the glass slide and the PDMS microchannel. During this process, mating surfaces are exposed to oxygen plasma generated at 80 watts and 20 sccm for 10 seconds. Exposure to the plasma chemically modifies the microchannel and electrode by inducing silanol and hydroxyl bonds at each surface [42]. As soon as a sample is removed from the plasma chamber, the exposed surfaces are aligned and mated as shown in Figure 8 (k). Upon contact, the two surfaces adhere forming a sealed device and the connecting ports are punched. Finally, the connecting ports are plumbed with capillary tubing in preparation for experiments as shown in Figure 12.

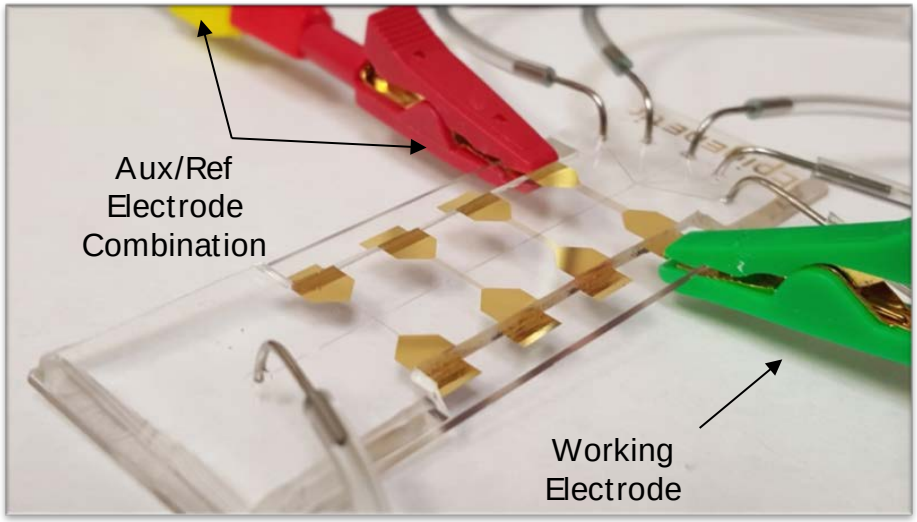

Figure 12: The completed device in the measurement configuration is shown with E1 positioned at the bottom and E4 connected with the potentiostat.

IV. EXPERIMENTAL RESULTS AND DISCUSSION

4.1 Experimental Set-Up and Constraints

Experimental trials are conducted using an eDAQ ZMAN Z100 electrochemical impedance analyzer in conjunction with an EA163 (eDAQ Inc., Colorado Springs, CO, 80916) potentiostat in the two-electrode configuration. The impedance analyzer, shown in Figure 13 (a), is used to analyze the electrochemical components within the cell that define charge transfer behavior. In the two electrode configuration, the reference and auxiliary electrode are connected in series opposite the working electrode as shown in Figure 13 (b).

When a potential is applied through the working electrode the ref/aux electrode combination collects the resultant current data. A loopback test is conducted to determine proper functionality of the impedance analyzer in which an arbitrary waveform is supplied to the input channels internally eliminating any signal from the potentiostat. Then the potentiostat is incorporated to ensure proper function of the network and create a phase shift calibration to remove system phase shift at high frequency.

A 5 kΩ resistor is assumed to have zero phase response over a 1 Hz-100 kHz spectrum and thus can be used to identify any noise introduced by the device network. These deviations are extracted from the signal by applying a minimized potential bias that eliminates phase shift at high frequencies. This phase correction is later used in the acquisition of data during the trials. The experimental operating frequency sweep is chosen by applying a preliminary sweep across the spectrum of device operation and selecting a frequency range that reflected a response to electric stimuli. Employing the parameters shown in Table 4.1, three progressive EIS experimental trials are conducted.

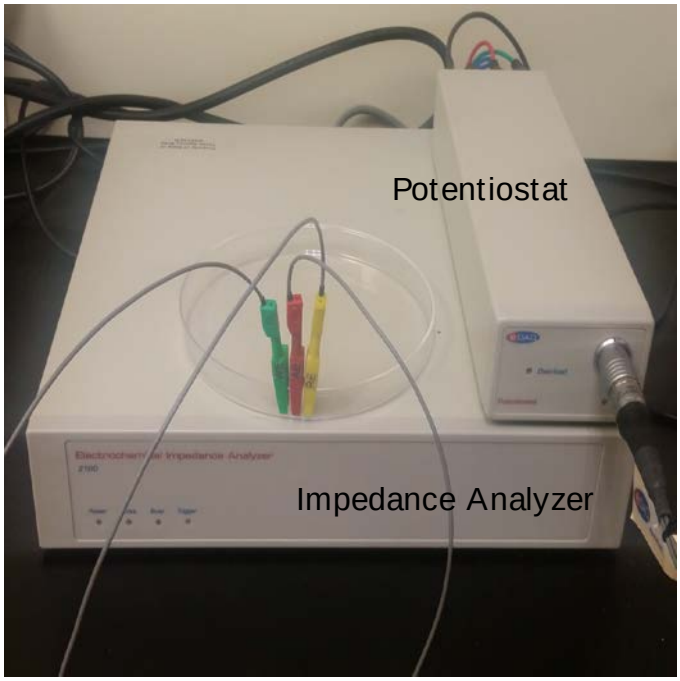

(a)

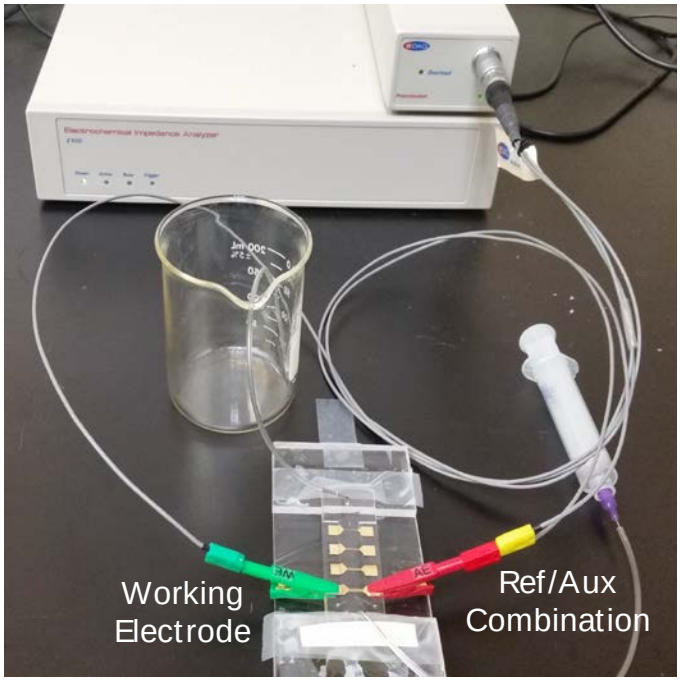

(b)

Figure 13: (a) The electrochemical impedance analyzer and potentiostat network. (b) The two electrode testing configuration with the reference and auxiliary electrodes connected in series.

Table 4.1. The parameters programmed into the potentiostat.

DC voltage	0 V
AC Amplitude (Excitation)	50 mV
Initial Frequency	500 Hz
Middle Frequency	15 kHz
High Frequency	30 kHz
Speed	Normal
Current	1 µA
Phase Correction	True

4.2 Solution Preparation

A continuous glucose monitoring system is required to sense changes in glucose levels frequently and accurately at a rapid rate. Thus, the sensing range of the system should be governed by physiological glucose readings. The lower threshold glucose level for diabetic patients is approximately 3.2 mM [51]. This research uses solutions below this threshold to develop a sensing modality to detect minute variations in glucose concentration. This enables detection of glucose changes at much lower concentrations to enhance device sensitivity and detection limits.

Solutions are prepared in ultra-pure DiH_2O (UPDI) that ranged from including 0M, 50 µM, 100 µM, 200 µM, 400 µM, 800 µM, 1.6 mM, and 3.2 mM. Using 450 g/L glucose (Item # G8769, Sigma-Aldrich Co, St. Louis, MO) and UPDI obtained from an ultrapure water system (Siemens LaboStar 2206-SW, Siemens Co., Munich, Germany) the solution is made. A 50 mL sample of UPDI is pipetted in 5 mL increments into a mixing vial where

exact glucose measurements are added. The solutions are ultrasonicated for a period of 5 minutes, separated into 5mL samples and allowed to acclimate to room temperature in dark storage over 2 hours. To minimize the effects of aging and exposure, testing is conducted within 24 hours of solution preparation with a single test conducted per vial of solution of a specified concentration.

4.3 Impedimeteric Response to Electrode Surface Area

The continuous glucose monitoring device is connected to a syringe with a glucose concentration at the inlet and a waste reservoir at the outlet filled with UPDI to pressurize the fluidic channel and eliminate solution backflow. Each glucose solution is applied to a target electrode array and the impedance spectra is collected over the course of 90 sampling measurements from low frequency to high frequency. Each interdigitated electrode (IDE) is tested at random and the trial is repeated a total of three times using three devices. The resultant data is stored via spreadsheets and loaded into ZMAN processing software.

In electrochemistry, electrode surface area is a significant aspect of impedimeteric response. Four IDEs are used to establish the effects of geometric modifications of electrode surface area: E1 with a single pair of IDE, E2 with three pairs of IDE, E3 with five pairs of IDE, and E4 with seven pairs of IDE as mentioned is chapter 3 section1. Figures 14 (a-d) demonstrate the Nyquist plot for each electrode ranging from 500 Hz to 35 kHz. A systematic decrease in cell impedance is observed as the number of interdigitated pairs increase. The addition of electrode pairs increases the surface area of the electrode hence enhancing electrode and analyte interaction.

At E1 the bulk of the reaction is driven by diffusion demonstrated by the pseudo-

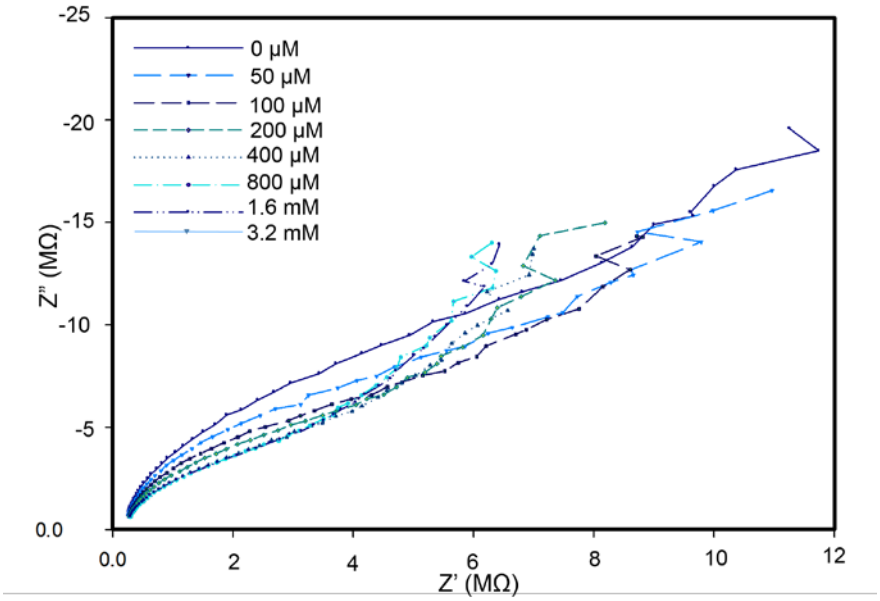

(a)

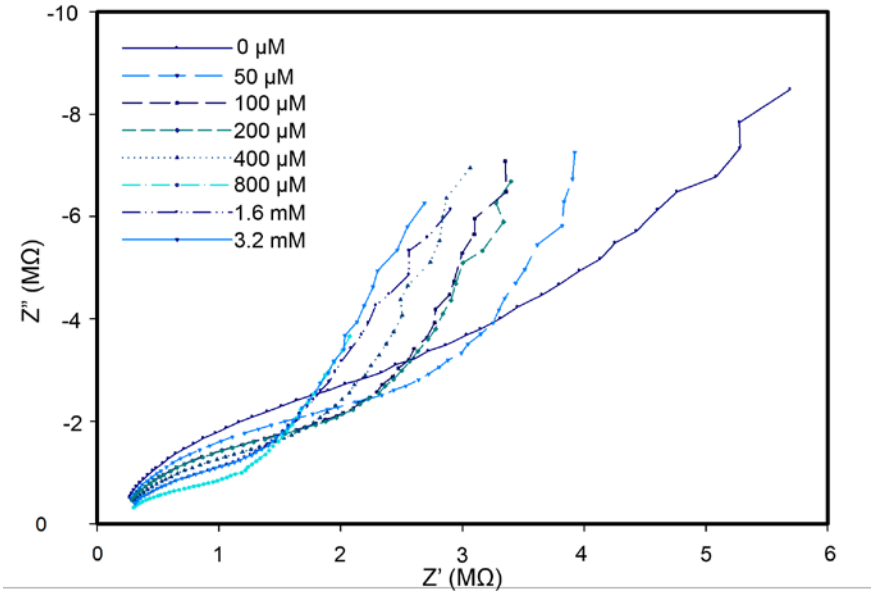

(b)

Figure 14: The Nyquist plot for (a) E1, (b) E2, (c) E3, and (d) E4.

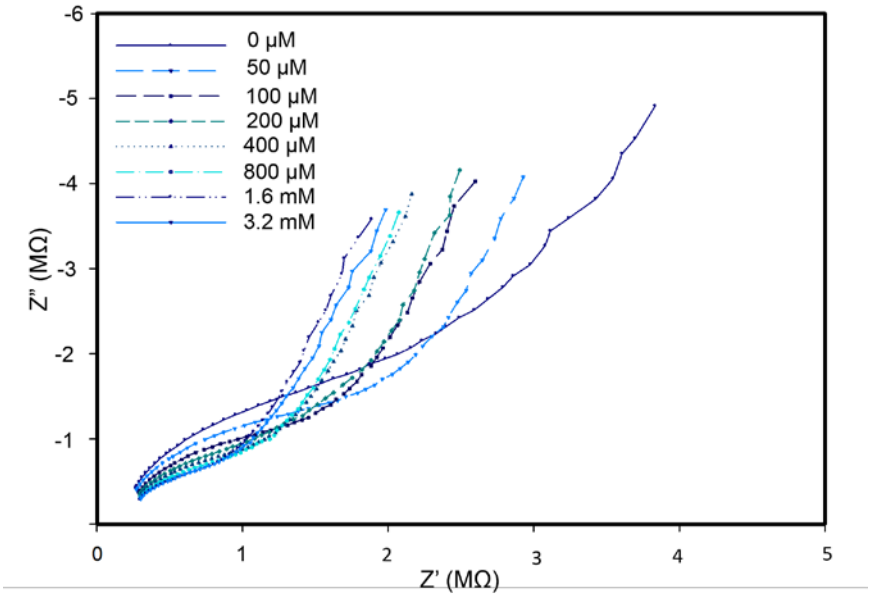

(c)

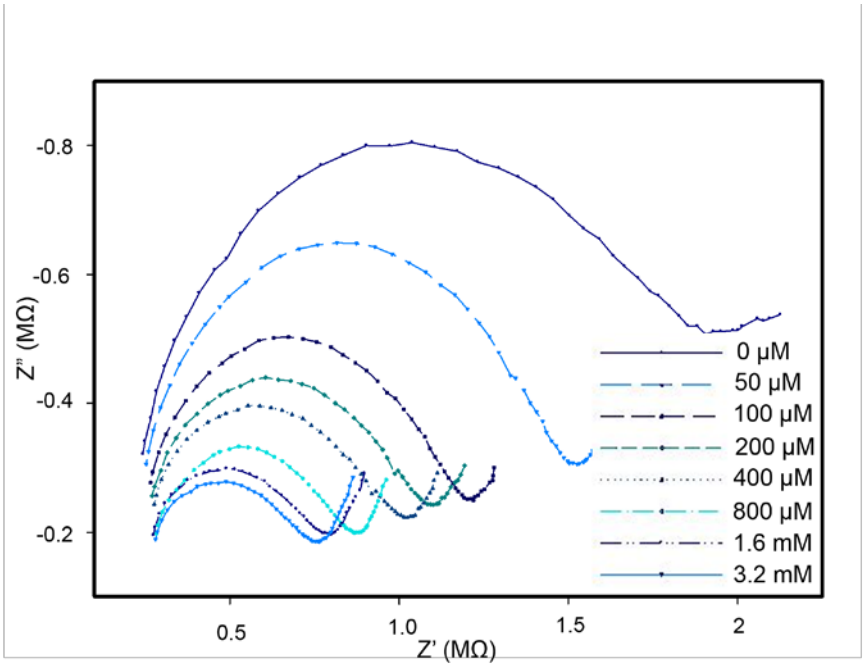

(d)

Figure 14 continued: The Nyquist plot for (a) E1, (b) E2, (c) E3, and (d) E4.

linear data at each glucose concentration. Higher frequencies induce kinetic electron transfer as evidenced by the parabolic curve shown in Figure 14 (a). Furthermore, concentrations above 200 µM, saturates the electrode set with solution molecules and the ability to decipher different concentrations of glucose is limited. The interaction of the electrode and electrolyte is constrained by the physical geometry of the cell. Since the interface is limited to two 100 µm x 50 µm areas, the reaction area is overwhelmed by molecules suspended in solution. While a sensing modality below 200 µM is possible in the diffusion-based portion of the impedance spectra, electrochemical diffusion is affected by a number of environmental conditions that are difficult to control such as temperature and atmospheric pressure. Hence, a fixed experimental methodology for continuous monitoring with diffusion driven reactions is difficult.

The impedimeteric responses at E2 and E3 are very similar to E1 with regard to the mechanism of electron transfer. Dominated by diffusion, E2 and E3 are also limited in their application in continuous monitoring modes. However, as shown in Figures 14 (b) and 14 (c), differentiation between solutions is increased with the addition of electrode pairs. Solutions as high as 800 µM are distinguished at 400 µM and E3 effectively identifies each solution concentration by descending impedance value.

At E4 there are seven IDE pairs and a different electrochemical behavior is observed. The diffusion effects are greatly reduced and kinetic electron transfer begins to drive the chemical reaction at a lower frequency in comparison to E1-E3. Based on the experiment, E4 provides sufficient bonding areas to not only discriminate between glucose concentrations, but also enhance device resolution as shown in Figure 14 (d). The increased dispersion between concentration plots indicates that interstitial glucose concentrations

could be deciphered. Figure 15 show the Nyquist plot of each electrode set at an 800 µM concentration. As the number of interdigitated electrodes increases, a decrease in impedance is exhibited. This is attributed to an effective dispersion of excitation potential over a surface area seven times the size of E1. The increase in physical dimensions of the electrode subsequently increases the electric field interacting with the target analyte.

As such, the target solution achieved an excitation state faster and displayed Faradic behavior that can be readily identified and analyzed. To confirm this behavior, impedance values of a 50 µM, 400 µM, and 3.2 mM solutions at each electrode array were plotted as a function of frequency as shown in Figure 16 (a). At E1-E3, the data exhibits dispersed frequency responses up to 10 kHz where the impedance signal began to converge asymptotically. E4, regardless of solution concentration, remained dispersed up to 15 kHz before approaching a fixed impedance value as shown in Figure 16 (b). As such, E4 is chosen to conduct the remainder of the experimental trials in this research.

4.4. Impedimeteric Response to Glucose Concentration

Since each array has a different surface area, variations in impedance are expected, but the resultant impedimetric responses at E1-E3 are shown to be diffusion driven. Hence, E4 is selected to conduct tests for device resolution as a function of glucose concentration as well as real time monitoring simulations. The Randles cell shown in Figure 5 (a) is chosen to model the behavior of the electrochemical cell. In enzymatic devices a constant phase element is generally required to describe the impedimetric response at the electrode/electrolyte interface due to adsorption phenomena. Since the bare gold electrodes do not rely on an enzymatic mediator to facilitate a chemical reaction, the electrochemical

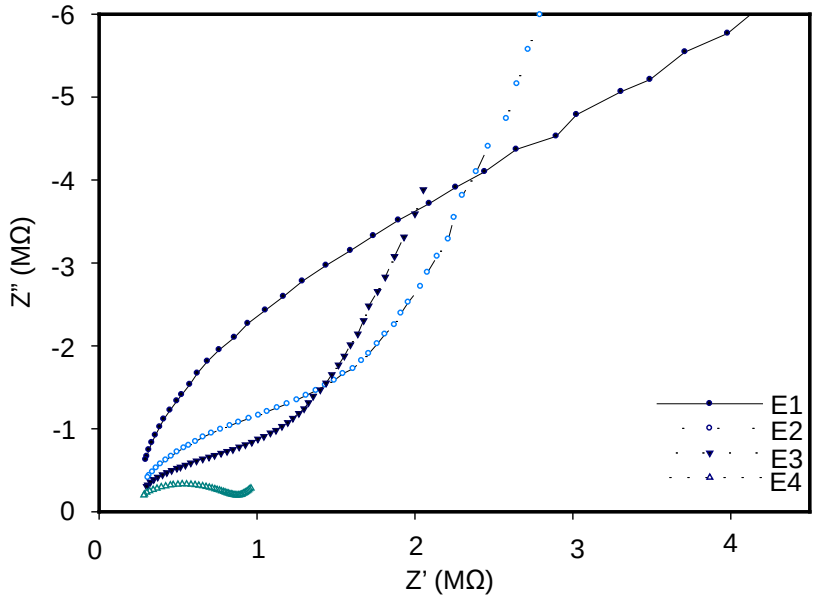

Figure 15: A Nyquist plot with each electrode array at 800 µM concentration. As electrode surface are is increased, the impedance response is decreased.

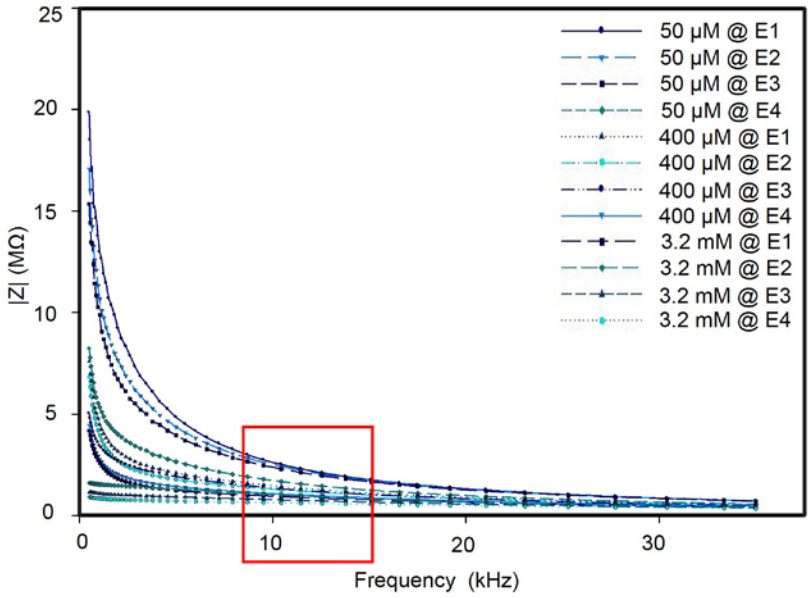

(a)

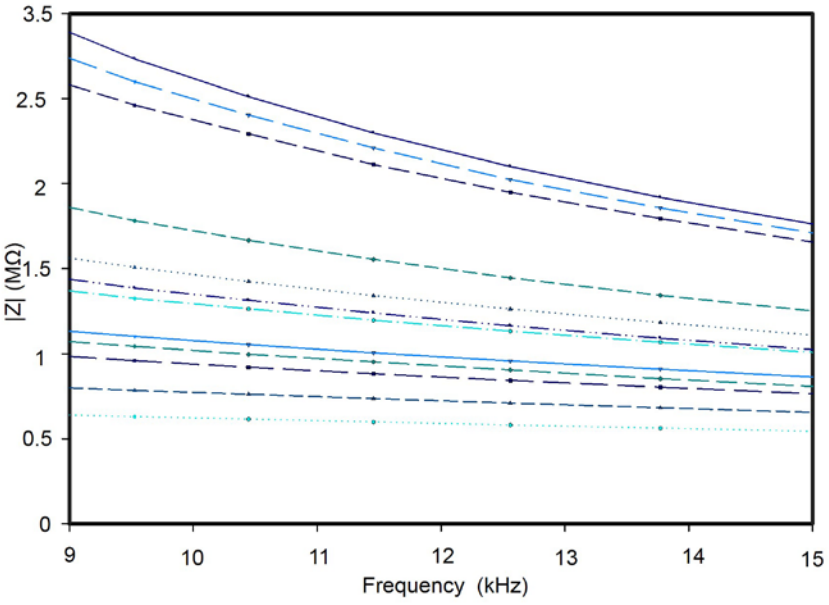

(b)

Figure 16: (a) Low (50 µM) medium (400 µM) and high (3.2 mM) concentrations at each electrode array are plotted as a function of frequency. (b) A magnified view of the area highlighted in red demonstrating the uniform dispersion at E4.

response is believed to be purely capacitive. Using ZMAN 2.2 data fitting software, two models are constructed to analyze the data. The first applied a constant phase element while the second used double layer capacitance. The Chi-squared values are measured and true double layer capacitance achieved a higher statistical score. Data fitting to the Randles model generated the results shown in Table 4.2.

Table 4.2: Equivalent circuit data obtained using ZMan 2.2 curve fitting software.

	Di H_2O	50 µM	100 µM	200 µM
R_{sol}	1.25E+05	1.64E+05	1.72E+05	1.70E+05
C_{dl}	1.45E-11	1.37E-11	1.51E-11	1.63E-11
R_{ct}	1.44E+06	1.23E+06	9.27E+05	7.90E+05
Z_w	-58.2505	-62.3765	-62.8655	-63.1815
	400 µM	800 µM	1.6mM	3.2mM
R_{sol}	1.78E+05	1.99E+05	1.80E+05	1.84E+05
C_{dl}	1.67E-11	2.00E-11	2.09E-11	2.07E-11
R_{ct}	7.47E+05	6.03E+05	5.21E+05	5.05E+05
Z_w	-63.655	-64.6925	-65.348	-67.2985

4.5 Concentration Sensitivity

A measurable response to changes in glucose concentration in aqueous solution is imperative to the development of continuous monitoring efforts. The discrete significance of glucose variation on the impedance spectra at E4 under the influence of equal experimental parameters is represented in the Nyquist plot shown in Figure 14 (d). The short linear response at low frequencies demonstrated the effects of Warburg impedance on the first time constant while the parabolic shape of each concentration characterized the effects of kinetic charge transfer.

Yoon states that the addition of glucose to ultrapure DI water does result in a decrease in impedance since the resistivity of water is effectively lowered by the addition of glucose [52]. This is explained by the chemical composition and interaction of both the solute and the solvent. In pure water, molecules generally do not possess sufficient free electrons to transfer current, but a process called auto-ionization occurs continuously in water to maintain an equilibrium state.

Molecular kinetics in H_2O generate sufficient forces to separate hydrogen atoms from water forming hydronium (H_3O^+) and hydroxide (OH^-) anions as shown in Figure 17 (a). H_3O^+ acts as an acid serving as a potential electron acceptor while OH^- behaves as an electron donor. These ions, while rare, do result in a current flow. Glucose exists in both a linear and cyclic form with aldehyde and hydroxyl functional groups around a carbon base. In the prevalent form, cyclic, carbon atoms form a ring as the terminal OH^- groups bond with the aldehyde group shown in Figure 17 (b). When glucose is added to water, functional groups in glucose are introduced to new bonding sites with H_3O^+ and OH^-. Since the hydronium achieved stability by bonding with glucose, the remaining hydroxyl group generated by auto ionization is free to serve as a charge carrier. In both glucose and water, covalent bonding holds the molecule together meaning that electrons are shared between atoms rather than being transferred from one atom to another resulting in a very stable bond that does not conduct electricity well. However, the aqueous solution is bonded together via weaker hydrogen bonds.

Glucose and water are polar molecules that orient themselves with respect to their opposite poles, and current flow results from the motion of electrically charged carriers in response to forces that act on them from an externally applied electric field. Under the

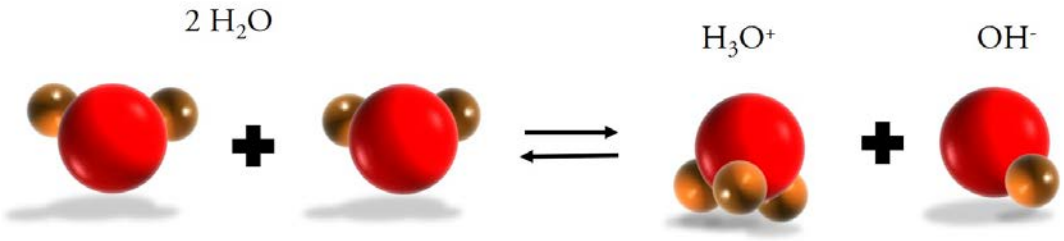

(a)

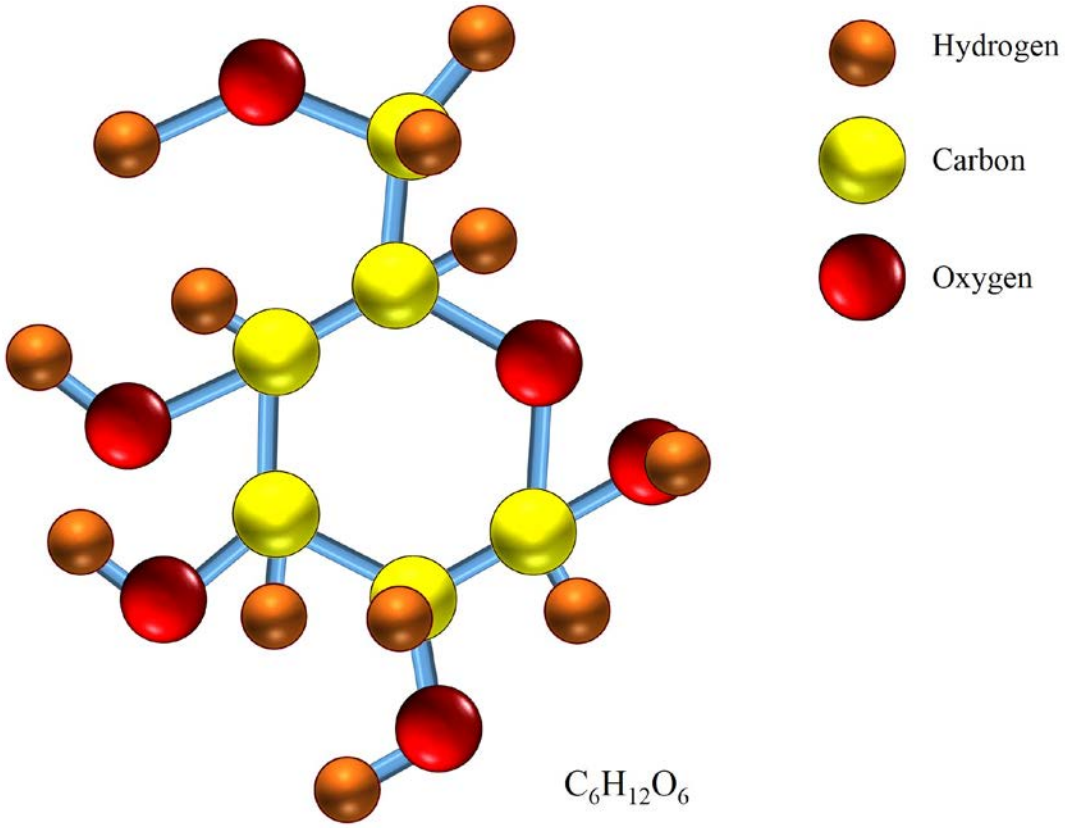

(b)

Figure 17: (a) The equilibrium reaction that generates ions in DI H_2O solutions is shown. (b) A 3-dimensional schematic of cyclic ring glucose is shown. Note the exterior hydroxyl groups and potential hydrogen bonding sites.

influence of an excitation voltage, the glucose and water molecules arranged themselves with respect to the potential applied at the cathode and the current response at the anode. Ions that are free or weakly bonded are attracted to their respective opposing polarities. The increase in glucose concentration increased the number of electron carriers and additional current flow paths are formed. A decrease in overall cell impedance is observed due to the increase in charge carriers.

4.6 Frequency Characterization for Real Time Glucose Monitoring

Variations in the impedance spectra are demonstrated when frequency is varied from 500 Hz to 35 kHz. In real time measurement, a fixed frequency parameter is required to ensure that the various concentrations are detected by the device. Figure 18 represents the impedance change as a function of the frequency at E4. Elevated frequencies had dramatic effects on the behavior of the electrochemical cell that are interpreted by the Randles analog. While charge transfer resistance and solution resistance remained unchanged, an increase in frequency resulted in an increase in the capacitive reactance demonstrated at the electrode/electrolyte interface (C_{dl}). Furthermore, these same frequency additions marginalized the effects of Warburg impedance, and reduced the Randles cell to effectively R_{sol} and R_{ct}. Since current flows through the path of least resistance, the bulk of the resultant current signal is obtained from the lower portion of the cell.

Convergence of the data to a lower impedimetric response is a direct reflection of the increase in frequency. Due to this effect, a frequency at the lower end of the spectrum is required. While the largest dispersion is demonstrated at 1 kHz, the signal to noise ratio

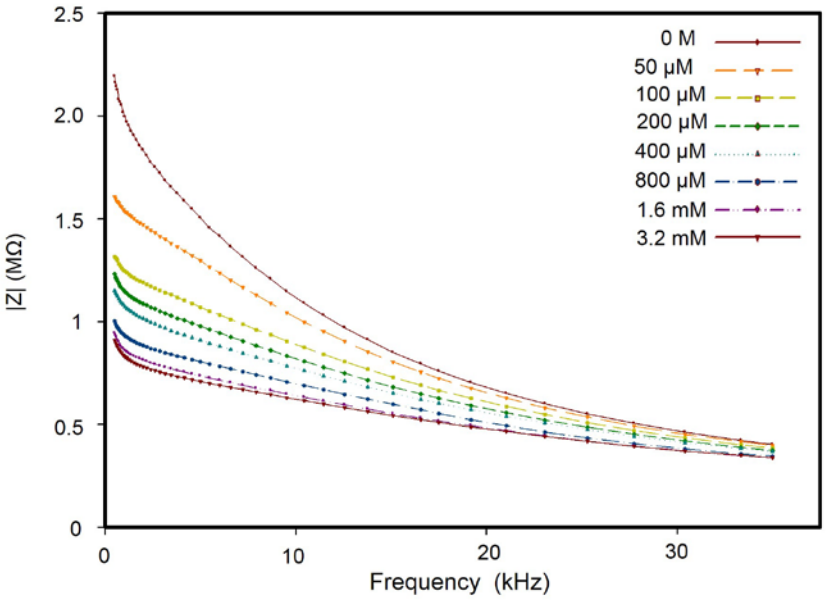

Figure 18: Impedance |Z| as a function of frequency at E4 for all concentrations of glucose. As frequency is increased the dispersion between glucose concentrations decreases.

in that range is comparably lower than that of 5 kHz and 10 kHz as demonstrated by the erratic impedance signal regardless of concentration shown in Figures 8 (a-c). 10 kHz is chosen because of the equidistant dispersion between concentrations when compared to data obtained at 5 kHz.

4.7 Continuous Glucose Monitoring

Continuous glucose monitoring methods have already been established implementing a variety of enzymatic techniques. Generally, these enzyme-based mediators drive chemical reactions within the cell generating the products of the reaction to be "sensed" by the device [53]. The inherent problems associated with enzymatic monitoring discussed in chapter 1 are compounded in real time monitoring scenarios. The fixed frequency impedimeteric testing method using a non-enzymatic bare gold electrode can be a viable solution.

The final experimental iteration is a real time glucose monitoring simulation in which the glucose concentration is varied over a period of 4.375 minutes at a sustained frequency of 10 kHz. The device is connected to three different glucose solutions including 50 µM, 400 µM, and 3.2 mM and the potentiostat and impedance analyzer are programmed with the aforementioned parameters. An impedance measurement is captured every 1.75 seconds with concentration changes in ascending order every 45 seconds. The glucose concentration is cycled for two iterations to establish signal reliability. This testing methodology provided insight into the device reaction time to deviations in glucose concentration as well as simulated continuous glucose monitoring.

A real time glucose monitoring modality is tested with the results given in Figure

19. A 50 µm solution is applied for the first interval of measurement generating a stable impedimeteric response of 1.04 MΩ that remains constant until the 400 µM solution is introduced into the channel. The increase in glucose concentration enables a rapid decrease in impedance to 752 kΩ where the signal remained until the final 3.2 mM solution is applied. In this case, the impedimeteric response reduces to 688 kΩ, a decrease in magnitude when compared to the impedance response from 50 µM to 400 µM. The validity of the device as a continuous glucose monitoring method is tested by repeating the cycle and observing the response. The impedance values for the second measurement iteration are 1.03 MΩ, 750 kΩ, and 685 kΩ respectively.

To establish a real time monitoring technique three critical metrics are considered, device sensitivity, response time, and reliability. Impedance data captured in real time demonstrates both sensing efficacy and device response to glucose variation. Although the impedance shift is reduced in magnitude, increases in concentration induce a rapid impedimeteric decrease. Deviations in magnitude are contributed to the glucose solution approaching saturation as concentration increased. The addition of glucose to water facilitates current flow through the solution from the working electrode to the reference electrode as previously discussed. As glucose increased, a steady reduction in impedance spectra is the response, but this behavior cannot be true for every increase in glucose concentration. Succinctly, the impedimeteric behavior of glucose in water must, at some point, converge on a single ohmic value as the solution approaches homogeneity.

The impedance response in this experiment suggests that as we approach the physiological lower glucose threshold of 3.2 mM for diabetes patients, the impedance value approaches a single impedance value. Tura discusses the impedance response at

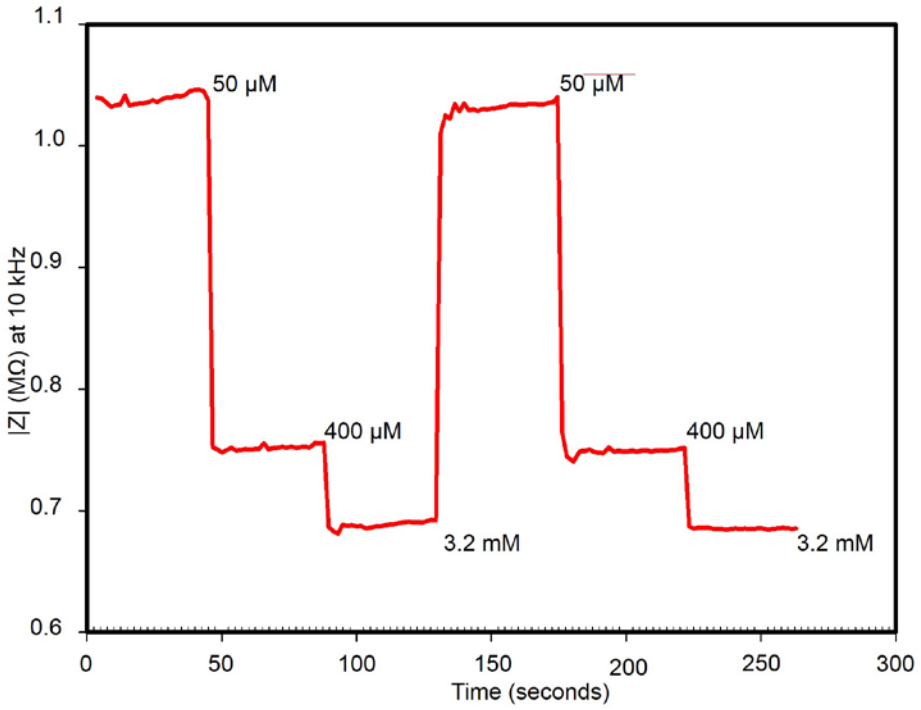

Figure 19: The step profile for continuous glucose monitoring at 50 µM, 400 µM, and 3.2 mM concentrations. The cyclic nature of the profile indicates device stability throughout the duration of the test.

physiological concentrations with a lower threshold of approximately 3.1 mM [54]. In their research, they state no impedance responses are detected at concentrations above this threshold in aqueous glucose solutions.

Another important element in continuous monitoring is device agility or ability to respond to changes in the solution. A distinct advantage of EIS is the ability to measure in the time domain allowing the calculation of discrete response time measurements. The sampling interval in this experiment is fixed for 150 measurements at 1.75 second intervals. The device is capable of detecting variations in glucose at a rate less than the measurement interval with an average response time of 1.7 seconds. The rapid response is attributed to the absence of a mediation layer. Mediated electrode devices have an inherently longer response time due to adsorption phenomena at the electrode/analyte interface. Conversely, the bare gold electrodes used in this study can interact with the solution upon contact. The absence of a mediator enabled the excitation of charge carriers and consequently rapid detection of concentration variations.

V. CONCLUSIONS

The research conducted reveals that EIS measurement coupled with a non-enzymatic gold electrode is an effective means of detecting variation in glucose concentration in aqueous solution. Iterative analysis of impedimeteric responses to electrode surface area, excitation frequency, and glucose concentration were investigated to establish a continuous glucose monitoring method.

Electrode arrays E1-E3 demonstrated reactions driven by diffusion until high frequency forced the reaction. E4 established an effective measuring modality demonstrating dispersion between glucose concentrations. It was shown that as glucose concentration increased, cell impedance decreased. Furthermore, the results suggest that device resolution increased as electrode surface area increased. Primary function of the device relied on the ability to sense variation in glucose concentration. Results suggest that the high resistivity of ultra-pure DI water was compromised by the addition of glucose. Repeated tests indicated that the addition of glucose molecules reduced impedance values by enriching the solution with ions that served as charge carries.

As glucose concentration increased charge transfer was increased. Real time experimental trials were conducted to establish viability of EIS technology as a means of sustained glucose monitoring. A five minute, 2 cycle iteration demonstrated stable impedance responses to glucose stimuli in 50 µM, 400 µM, and 3.2 mM concentrations with impedance values of 1 MΩ, 750 kΩ, and 685 kΩ, respectively.

While this research established validity of the experimental method, there are still many obstacles on the path to an effective continuous glucose monitoring technique. One of the most prominent issues is the nature of biological systems. The solution under

investigation was a mixture of UPDI water devoid of ionic contaminants, and glucose. Generally, biological fluids are full of chemical compounds, salts, and other ions that must be distinguished and understood to advance the technology to an in-vitro application.

VI. FUTURE WORK

Recent works show that impedimetric response above the physiological threshold in aqueous glucose solutions is negligible. However, a continuous glucose device does not require sensing above the threshold provided a metric can be established at a fixed set of testing parameters. The fixed impedance values in the continuous glucose monitoring experiment illustrate feasibility of this concept. If the impedance value is repeated over time as shown, then a theoretical baseline could be applied to the data such that only the variation from an impedimetric baseline is detected. This baseline could be implemented to establish an upper and lower tolerance limit for acceptable glucose levels in the system.

The two electrode configuration successfully demonstrated the ability to sense variation in glucose concentration at concentrations below 3.2 mM. At the upper threshold the dispersion between concentrations dissipated. A viable solution is the addition of a dedicated auxiliary electrode that can monitor electrochemical phenomena in the solution while isolated from any excitation potential. Smaller electrode surface areas were subject to saturation. A new interdigitated electrode design that maximizes electrode/analyte interaction by maximizing electrode geometry could yield significant results.

The nature of this testing methodology has many other potential applications. The microfluidic platform in this research is a stepping stone in the development of a diagnostic platform capable of diagnosing and detecting a variety of analytes by modifying the electrode surface and experimental parameters.

REFERENCES

[1] W. Jung, H. Jungyoup, C. Jin-Woo and C. H. Ahn, "Point-of-care testing (POCT) diagnostic systems using microfluidic lab-on-a-chip technologies," *Microelectronic Engineering,* pp. 46-57, 2014.

[2] J. P. Lafleur, J. Alexander, S. Silja and J. P. Kutter, "Recent advances in lab-on-a-chip for biosensing applications," *Biosensors and Bioelectronics,* pp. 213-233, 2016.

[3] A. Chaubey and B. Malhotra, "Mediated Biosensors," *Biosensors and Bioelectronics,* pp. 441-456, 2002.

[4] L. Clark and C. Lyons, "Electrode systems for continuos monitoring in cardiovascular surgery," *Annals of the New York Academy of Sciences,* pp. 29-45, 1962.

[5] S. Vigneshvar, C. Sudhakumari, B. Senthilkumaran and a. H. Prakash, "Recent advances in biosensor technology for potential applications - an overview," *Frontiers in Bioengineering and Biotechnology*, pp. 1-9, 2016.

[6] S. Sang, Y. Wang, Q. Feng, Y. Wei, J. Ji and W. Zhang, "Progress of new label-free techniques for biosensors: a review.," *Critical reviews in biotechnology,* pp. 465-481, 2016.

[7] D. Dey and T. Goswami, "Optical biosensors: a revolution towards quantum nanoscale electronics device fabrication," *BioMed Research International*, 2011.

[8] J. Yang, T. Ono and M. Esashi, "Mechanical behavior of ultrathin microcantilever," *Senors and Actuators A: Physical,* pp. 102-107, 2000.

[9] J. Arlett, E. Myers and M. Roukes, "Comparative advantages of mechanical biosensors," *Nature Nanotechnology* , pp. 1-28, 2011.

[10] R. Shervedani, M. A.H. and N. Zamiri, "A novel method for glucose determination based on electrochemical impedance spectroscopy using glucose oxidase self-assembled biosensor.," *Bioelectrochemistry,* pp. 201-208, 2006.

[11] A. Chauby and B. Malhotra, "Mediated Biosensors.," *Biosensors and Biolelectronics,* pp. 441-56, 2002.

[12] D. Grieshaber, R. MacKenzie, J. Vörös and E. Reimhult, "Electrochemical Biosensors - Sensor Principles and Architectures," *Sensors,* pp. 1400-1458, 2008.

[13] D. Buerk, Biosensors. Theory and Applications, Lancaster, PA: Technomic Publishing, 1993.

[14] N. Sheppard, R. Tucker and C. Wu, "Electrical Conductivity Measurements Using Microfabricated Interdigitated Electrodes," *Analytical Chemistry* , pp. 1199-1202, 1993.

[15] American Diabetes Association, "Tight Diabetes Control," 13 May 2015. [Online]. Available: http://www.diabetes.org/living-with-diabetes/treatment-and-care/blood-glucose-control/tight-diabetes-control.html?referrer=https://www.google.com/.

[16] International Diabetes Federation, "Diabetes Facts and Figures," 2015. [Online]. Available: http://www.idf.org/about-diabetes/facts-figures. [Accessed 18 June 2016].

[17] D. Spero, "Diabetes Self-Management," 28 September 2011. [Online]. Available: http://www.diabetesselfmanagement.com/blog/is-continuous-glucose-monitoring-worth-it/. [Accessed 12 June 2016].

[18] J. Wang, "Electrochemcial Glucose Biosensors," *Chemical Review* , pp. 814-825, 2008.

[19] S. Park, H. Boo and T. D. Chung, "Electrochemical non-enzymatic glucose sensors," *Analytica Chimica Acta*, pp. 46-57, 2006.

[20] S. J. Lee, H. S. Yoon, X. Xuan, J. Y. Park, S.-J. Paik and M. G. Allen, "A patch type non-enzymatic biosensor based on 3D SUS micro-needle electrode array for minimally invasive continuous glucose monitoring," *Sensors and Actuators B: Chemical*, pp. 1144-1151, 2016.

[21] D. Pletcher, "Electrocatalysis: present and future," *Journal of Applied Electrochemistry* , pp. 403-415, 1984.

[22] W. Dong, J. Luo, H. He and L. Jiang, "A reinforced composite structure composed of polydiacetylene assemblies deposited on polystyrene microspheres and its application to H5N1 virus detection," *International Journal of Medicine*, pp. 221-232, 2013.

[23] Y.-J. Lee, D.-J. Park, J.-Y. Park and Y. Kim, "Fabrication and Optimization of a Nanoporous Platinum Electrode and a Non-enzymatic Glucose Micro-sensor on Silicon," *Sensors*, pp. 6154-6164, 2008.

[24] M. Pasta, F. L. Mantia and Y. Cui, "Mechanism of glucose electrochemical oxidation on gold surface," *Electrochimica Acta,* pp. 5561-5568, 2010.

[25] Y. Li, Y.-Y. Song, C. Yang and X.-H. Xia, "Hydrogen bubble dynamic template synthesis of porous gold for nonenzymatic electrochemical detection of glucose," *Electrochemistry Communications,* pp. 981-988, 2007.

[26] E. H. El-Ads, A. Galal and N. F. Atta, "Electrochemistry of glucose at gold nanoparticles modified graphite/SrPdO3 electrode – Towards a novel non-enzymatic glucose sensor," *Journal of Electroanalytical Chemistry,* pp. 42-52, 2015.

[27] Y. Siti Nur Akmar Mohd, I. M. Isa and N. Hashim, "Novel alkaline-reduced cuprous oxide/graphene nanocomposites for non-enzymatic amperometric glucose sensor application," *Materials Science and Engineering: C,* pp. 465-473, 2016.

[28] Z.-x. Cai, C.-c. Liu, G.-h. Wu, X.-m. Chen and X. Chen, "Palladium nanoparticles deposit on multi-walled carbon nanotubes," *Electrochimica Acta,* pp. 756-762, 2009.

[29] M. M. Rahman, A. J. S. Ahammad, J.-H. Jin, S. J. Ahn and J.-J. Lee, "A Comprehensive Review of Glucose Biosensors Based on Nanostructured Metal-Oxides," *Sensors,* pp. 4855-4886, 2010.

[30] H. Yang and Y. Zhu, "Size dependence of SiO 2 particles enhanced glucose biosensor," *Talanta,* pp. 569-574, 2006.

[31] Y. Zhonga, T. Shia, Z. L. b, S. Cheng, Y. Huang, X. Tao, G. Liao and Z. Tang, "Ultrasensitive non-enzymatic glucose sensors based on different copper oxide nanostructures by in-situ growth," *Sensors and Actuators B: Chemical,* pp. 326-333, 2016.

[32] K. Ghanbari and Z. Babaei, "Fabrication and characterization of non-enzymatic glucose sensor based on ternary NiO/CuO/polyaniline nanocomposite," *Analytical Biochemistry,* pp. 37-46, 2016.

[33] J. Chung, J. S. Kang, J. SooJurng, J. HeeJung and B. C. Kim, "Fast and continuos microorganism detection using aptamer-conjugated flourescent nanoparticles on an optofluidic platform," *Biosensors and Bioelectronics,* pp. 303-308, 2015.

[34] A. A. Ensafi, N. Zandi-Atashbar, B. Rezaei, M. Ghiaci and M. Taghizadeh, "Silver nanoparticles decorated carboxylate functionalized SiO2, New nanocomposites for non-enzymatic detection of glucose and hydrogen peroxide," *Electrochimica Acta,* pp. 208-216, 2016.

[35] R. A. Soomro, O. P. Akyuz, R. Ozturk and Z. H. Ibupoto, "Highly sensitive non-

enzymatic glucose sensing using gold nanocages as efficient electrode material," *Sensors and Actuators B: Chemical,* pp. 230-236, 2016.

[36] H. Li, C.-Y. Guo and C.-L. Xu, "A highly sensitive non-enzymatic glucose sensor based on bimetallic Cu–Ag superstructures," *Biosensors and Bioelectronics,* pp. 339-346, 2015.

[37] A. Lasia, "Electrochemical impedance spectroscopy and its applications," in *Modern aspects of electrochemistry*, Springer, US , 2002, pp. 143-248.

[38] E. Barsoukov and R. J. Macdonald, Impedance Spectroscopy Theory, Experiment, and Applications, Hoboken, NJ: John Wiley @ Sons Inc., 2005.

[39] R. Shervedani, A. Mehrjardi and N. Zamiri, "A novel method for glucose determination based on electrochemical impedance spectroscopy using glucose oxidase self-assembled biosensor," *Bioelectrochemistry,* pp. 201-208, 2006.

[40] C. M. Martinez, E. Treo, R. Madrid and C. Felice, "Real-time measurement of glucose using chrono-impedance technique on a second generation biosensor," *Biosensors. Bioelectronics,* pp. 200-203, 2011.

[41] B. Y. Chang and S. M. Park, "Electrochemical Impedance Spectroscopy," *Annual Review of Analytical Chemistry,* pp. 207-229, 2010.

[42] H. Li, J.-h. Jang and a. S.-x. Cai., "Fabrication of microfluidic systems in poly (dimethylsiloxane)," *Polym. Bull 1,* 2005.

[43] L. Yang and R. Bashir, "Electrical/electrochemical impedance for rapid detection of foodborne pathogenic bacteria," *Biotechnology advances,* pp. 135-150, (2008).

[44] P. Ihalainen, F. Pettersson, M. Pesonen, T. Viitala, A. Määttänen, R. Österbacka and J. Peltonen, "An impedimetric study of DNA hybridization on paper-supported inkjet-printed gold electrodes.," *Nanotechnology,* p. 094009, (2014).

[45] D. C. Vanegas, Y. Rong, N. Schwalb, K. D. Hills, C. Gomes and E. S. McLamore, "Rapid detection of listeria spp. using an internalin A aptasensor based on carbon-metal nanohybrid structures," *SPIE Sensing Technology+ Applications,* pp. 948708-948708, 2015.

[46] K. Tsugimura, H. Ohnuki, H. Endo, D. Tsuya and M. Izumi, "Protein-G-based human immunoglobulin G biosensing by electrochemical impedance spectroscopy.," *Japanese Journal of Applied Physics,* p. 02BE06, 2016.

[47] H. Wang, H. Ohnuki, H. Endo and M. Izumi, "Impedimetric and amperometric

bifunctional glucose biosensor based on hybrid organic–inorganic thin films.," *Bioelectrochemistry*, pp. 1-7, 2015.

[48] Gamry Instruments, "Basics of Electrochemical Impedance Spectroscopy," 2016. [Online]. Available: http://www.gamry.com/application-notes/EIS/basics-of-electrochemical-impedance-spectroscopy/.

[49] X.-Z. Yuan, C. Song, H. Wang and J. Zhang, Electrochemical Impedance Spectroscopy in PEM Fuel Cells, London: Springer, 2010.

[50] J. McDonald, D. Duffy, J. Anderson, D. Chiu, H. Wu, O. Schueller and G. Whitesides, "Fabrication of microfluidic systems in poly(dimethylsiloxane)," *Elecctrophoresis*, pp. 27-40, 2000.

[51] The American Diabetes Association, "Checking Your Blood Glucose," 3 March 2015. [Online]. Available: http://www.diabetes.org/living-with-diabetes/treatment-and-care/blood-glucose-control/checking-your-blood-glucose.html. [Accessed 2 August 2016].

[52] G. Yoon, "Dielectric properties of glucose in bulk aqueous solutions: Influence of electrode polarization and modeling," *Biosensors and Bioelectronics,* pp. 2347-2353, 2011.

[53] A. Turner, "Biosensors: sense and sensiblity," *Chemical Society Review* , pp. 3184-3196, 2013.

[54] A. Turaa, S. Sbrignadelloa, S. Barisonb, S. Contic and G. Pacinia, "Impedance spectroscopy of solutions at physiological glucose concentrations," *Biophysical Chemistry*, pp. 235-241, 2007.